SPIRAL II : Preliminary design study

G. de Angelis, S. Brandenburg, Ph. Dessagne, J.P. Gatesoupe, W. Gelletly, M. Huyse, B. Jonson, J. Martino, W. Mittig, Yu.Ts. Oganessian, et al.

November 28, 2001

SPIRAL II : Preliminary Design Study

There is currently in the nuclear physics community a strong interest in the use of beams of accelerated radioactive ions. Although a fast glance at the nuclide chart immediately shows the vast unknown territories on the neutron-rich side of the valley of beta stability, only few projects are concerned with the neutron-rich nuclides. The SPIRAL-II program aims at studying the techniques for delivering beams of neutron-rich radioactive nuclides at energies of a few MeV per nucleon. This energy allows to overcome the Coulomb repulsion between the radioactive beam and the target nuclei in most systems and opens up new possibilities for experimental studies of neutron-rich nuclei and of the synthesis of the heaviest elements. A number of new phenomena are indeed predicted to occur in nuclei with large neutron excess which will help to improve nuclear models by comparison with data not available to date. Moreover, it can be noted that the astrophysics community is very interested in nuclear data for calculations of nucleosynthesis.

The scientific council of GANIL asked to perform a comparative study on the production methods based on gamma induced fission and rapid-neutron induced fission concerning the nature and the intensity of the neutron-rich products. The production rate expected should be around 10^{13} fissions per second. The study should include the implantation and the costs of the concerned accelerators. The scientific committee recommended also to study the possibility to re-inject the radioactive beams of SPIRAL II in the cyclotrons available at GANIL in order to give access to an energy range from 1.7 to 100 MeV/nucleon

For that purpose, some study groups have been formed to evaluate the possibility of such a project in the different components: physics case, target-ion sources, drivers, postacceleration and general infrastructure. The organization of the project study is given at the end of this report. You will find also the name of all the people involved in the study.

The following report presents an overview of the study.

The physics case of SPIRAL2

The SPIRAL2 facility of GANIL is supposed to deliver high-intensity beams of neutron- rich fission fragments. The use of these high-intensity beams at the GANIL low-energy ISOL facility or their acceleration to a few tens of MeV/nucleon opens new possibilities in nuclear structure physics, nuclear astrophysics, as well as in reaction dynamics studies.
A few of these nuclear physics related subjects will be described here.

Towards the neutron drip line

The existence of an atomic nucleus defined by its stability with respect to the strong interaction is probably its most basic feature. The limit of stability of neutron-rich nuclei, the neutron drip line, has up to now been experimentally reached only up to oxygen (Z=8). SPIRAL2 beams should allow to go to higher-Z elements and to test the limits of stability for these elements. These studies can be conducted by accelerating and fragmenting neutron-rich fission products in projectile fragmentation-type experiments.
Even if the neutron drip line is out of reach for elements above Z=14 or so, projectile fragmentation of neutron-rich nuclei is an interesting way to produce very neutron-rich nuclides. As an example, doubly-magic ^{78}Ni may be produced via projectile fragmentation of ^{82}Ge fission fragments. In a similar way, ^{110}Zr can be produced from ^{114}Ru secondary beams. Rough estimates show that the loss in intensity of secondary fission-fragment beams as compared to stable primary beams may be overcompensated by the higher fragmentation cross sections. In selected cases, this should yield counting rates of exotic fragments one or two orders of magnitude higher than reached by stable-beam projectile fragmentation. These types of studies need rather high beam energies for the fission fragments of about 50-70 MeV/nucleon.
Decay studies with these neutron-rich isotopes will allow for many interesting studies. In particular, neutron-neutron correlation studies in beta-delayed two-neutron emission will enable us to determine the time scale of the neutron emission and the size of the emitting source.
The comparison between experiment and theory, in particular for the location near or in the "island of inversion" (N~20), of Gamow Teller (GT) and natural parity states fed in beta decay, has allowed to obtain crucial information on the neutron-neutron and proton-neutron interaction in the involved subshells. In this context it would be of prime interest to explore other mass regions near the shell closures (e.g. Z ~40, 50 and N ~50).

Single-particle levels and spin-orbit splitting around ^{132}Sn

The shell-model description of the structure of the atomic nucleus is based on a picture where all the nucleons are arranged in shells, each capable of containing a maximum number of nucleons. These shells corresponding to magic nucleon numbers are well established at the stability line and for radioactive nuclei close to stability. However, it is not possible to predict how this shell

structure evolves far from stability. In particular, it has been shown that, for neutron-rich isotopes around the classical shell closures at N=20 and N=28, the shell gap between two major shells is either strongly reduced or intruder configurations become very important.
SPIRAL2 is the ideal facility to study the N=82 shell closure over a wide variety of nuclei. As shown in figure 1, only a few single-particle levels are known in the ^{132}Sn region. These single-particle energies are crucial inputs for shell-model studies. With SPIRAL2 the evolution of the single-particle levels can be studied for example with transfer reactions involving medium-energy beams of nuclei along the Z=50 closed proton shell or the N=82 neutron shell.
A related topic is the study of the spin-orbit splitting e.g. of the $\pi h_{9/2}$ and the $\pi h_{11/2}$ as well as the $\pi g_{7/2}$ and the $\pi g_{9/2}$ orbits. According to certain model predictions, the energy splitting of these spin-orbit partners should decrease or even vanish far from stability for very neutron-rich isotopes. To extend our knowledge on the spin-orbit splitting far beyond the doubly-magic nucleus ^{132}Sn is a prime subject for SPIRAL2.

.

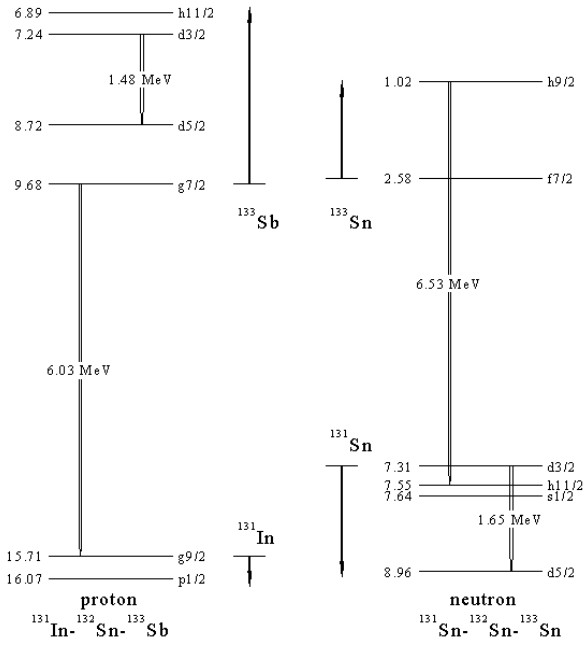

Figure 1: Experimentally known proton and neutron single-particle energies in the ^{132}Sn region.

Shell closure far from stability and new shell gaps

As mentioned in the previous section, far from stability the classical shell gaps might vanish and new magic numbers may show up. These new magic numbers could be those predicted by a harmonic oscillator shell model when switching off the spin-orbit coupling.
In this case, the neutron and proton numbers 40 and 70 become magic and large shell gaps are predicted.
These predictions can be tested by measuring the collectivity in nuclei around N,Z = 40, 50, 70. For example, ^{60}Ca is one of these nuclei of interest with a magic proton number Z=20 and a possible shell closure at N=40. Other regions of interest are ^{78}Ni with "classical" magic numbers or ^{110}Zr with N=70 and Z=40.
An elegant way of studying the collectivity of these nuclei and their neighbors is Coulomb excitation. With counting rates as low as ten particles per second and energies around 30-50 MeV/nucleon, the position of the first excited 2^+ state and the excitation strength, the B(E2) value, can be determined by measuring the rays from these nuclei after Coulomb excitation. This type of experiments allow for a rather quick "mapping" of a region of interest. As an example, figure 2 shows the evolution of the 2^+ state energy for nickel isotopes.

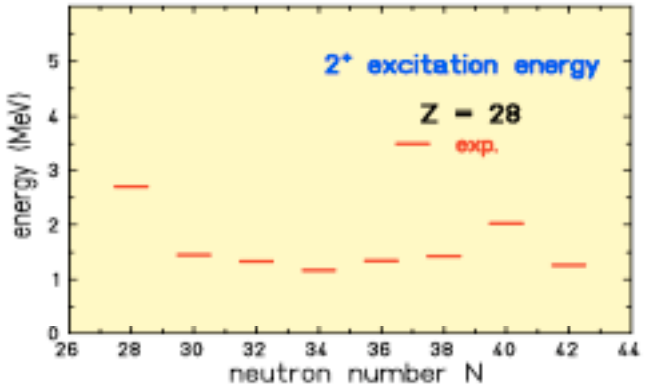

Figure 2: Energy of the first excited 2^+ states in even-even nickel nuclei. The shell and sub-shell closures at N=28 and N=40 are clearly evidenced by the increase of the 2^+ energies.

Similar studies can be conducted with even lower counting rates by using beta decay as a probe. The structure of ^{78}Ni can be studied at the GANIL low-energy facility via beta decay of ^{78}Co or after beta-delayed neutron emission from ^{79}Co. In the same way, ^{110}Zr is accessible via the decays of ^{110,111}Y. Another proposal is to study the robustness of the Z=50 shell far from stability via the beta decay of indium isotopes. The Z=50 shell closure creates an 8^+ isomer in $^{98}_{48}Cd$ which, if the Z=50 closure persists, should also show up in $^{130}_{48}Cd$.
Finally, mass measurements also give crucial indications of shell behaviour from the two-neutron separation energies.

Static nuclear moments far from stability

The measurement of the nuclear quadrupole and magnetic moments allow for a detailed study of the nuclear structure of the atomic nucleus. They give access to quantities like the nuclear g factor as well as the deformation of a nucleus.
With radioactive beams, these studies can be performed either by using directly the high-energy radioactive beam, polarizing it by means of the tilted-foil method, or by introducing the polarization or orientation needed for the measurements by reactions of the secondary beams. These reactions can be of the fusion-evaporation type to study properties of isomers populated in these reactions or fragmentation reactions to study ground-state properties.
Figure 3 shows a measurement recently performed at the LISE 3 separator of GANIL using the Time Differential Perturbed Angular Distribution (TDPAD) method to determine the properties of an $I^{\pi} = 9/2^{+}$ isomer in ^{67}Ni. The experiment allowed to determine the g-factor of this isomeric state and to compare it to shell model calculations, constraining in this way the theoretical possibilities to describe this nucleus. So far the TDPAD method is the only way to study g-factors of isomers in neutron-rich nuclei having life-times between 100 ns and 50 μs. Similar studies can be performed on other magic or semi-magic nuclei accessible with SPIRAL2.

Another interesting possibility for nuclear moments of exotic nuclei is to use the powerful method of laser spectroscopy which has the bonus of providing information on the mean-square charge radius.

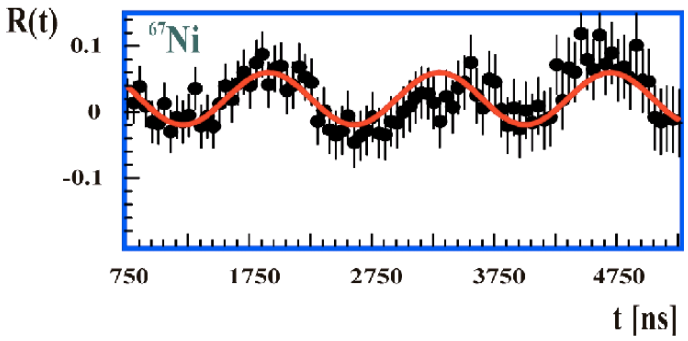

Figure 3: g-factor determination of an $I^{\pi} = 9/2^{+}$ isomer in ^{67}Ni. The ion arrival time was used as time t=0 to measure the isomeric decay on top of which the anisotropic oscillation is present. The oscillation pattern R(t) of the isomeric β-decay is proportional to the isomeric g-factor.

High-spin states produced with fission fragments

Superdeformed states have been identified in a large number of nuclei. However, as basically all these studies have been conducted with stable-beam/stable-target combinations, superdeformed states have been studied mainly in stable or proton-rich nuclei.
Only a few additional studies were carried out with deep inelastic reactions to investigate high-spin states in somewhat neutron-rich nuclei. Using neutron-rich beams to induce fusion-evaporation reactions will open completely new possibilities for the investigation of high-spin states in medium- and heavy-mass neutron-rich or stable nuclei. The excess of neutrons as compared to stable-beam induced reactions will increase the fission barrier of the compound nuclei and thus dramatically increase the survival probability. Figure 4 shows the influence of the neutron excess on the fission barrier. Hyperdeformation is predicted by HFB calculations around N=108. The isotopes of

interest (^{176}Er, ^{178}Yb, ^{180}Hf) can be produced by ^{130}Cd, ^{132}Sn, and ^{134}Te induced reaction, respectively, on a ^{48}Ca target and studied with devices like EUROBALL or EXOGAM.

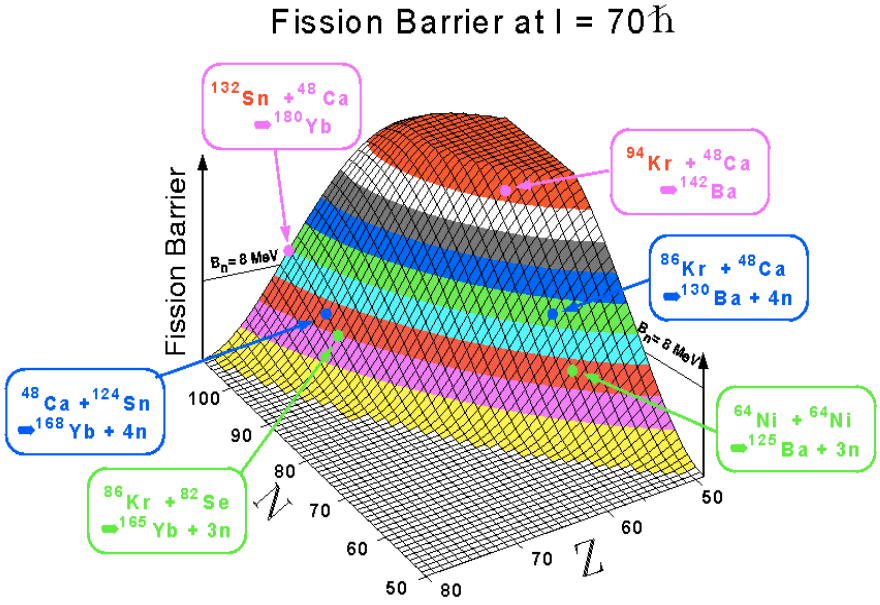

Figure 4: Fission barrier as a function of the mass number A and the charge number Z of the compound nucleus. Several reactions with stable and neutron-rich beams are compared showing the influence of the neutron excess on the fission barrier

.

Figure 5 shows the potential energy for ^{174,176}Eu as a function of the deformation parameter beta**.**

Another topic of interest are nuclei like ^{144}Xe. This nucleus is predicted to have a sizeable neutron skin. High-spin states and thus rotation of such a neutron-skin nucleus has never been observed and might give new insight into its structure and in particular into the influence of the neutron skin on the rotational behavior of such nuclei.

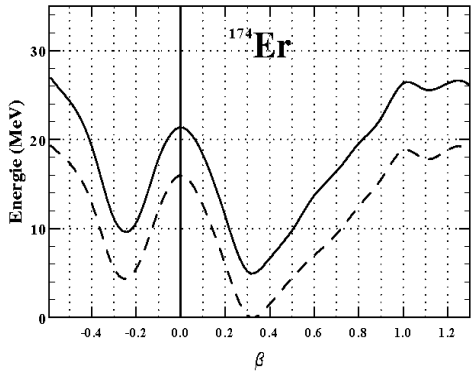

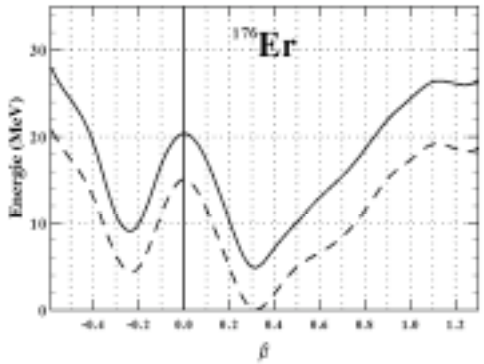

Figure 5: Potential energy as a function of the deformation parameter b for ^{174,176}Eu as determined by HFB calculations.

Heavy nuclei far beyond the heaviest naturally occuring element uranium have been studied recently in Argonne and in Jyväskylä by fusion-evaporation reactions with stable beams and targets. More neutron-rich very heavy ions may be produced by fusion reactions with radioactive fission fragments. For example, heavy nobelium or seaborgium isotopes can be produced by ^{132}Sn induced reactions on ^{130}Te and ^{138}Ba targets. With SPIRAL2, the resulting ^{260}No and ^{268}Sg can be e.g. detected with VAMOS using the recoil-decay-tagging method and the rays can be observed with the new EXOGAM device. Other nuclei may be produced with different beam/target combinations.

Search and production of super-heavy nuclei

Isotopes above proton numbers of about Z=106 are only stable or quasi-stable with respect to the strong interaction due to the shell structure of the atomic nucleus. Without the additional binding energy gain from the stabilizing effect of the nuclear shells, these nuclei would not exist. Super-heavy elements have been produced with proton numbers up to Z=112 and perhaps as far as Z=116.

Beyond the observation and identification of new chemical elements, one of the interests of the production of super-heavy isotopes is the search of new shell closures for these high- Z elements. According to different model predictions, the next neutron shell is expected at N=184. However, for the next proton shell gap, the predictions are less clear. Depending on the model, shell closures are expected at Z=114, 120, or 126.

With stable beams, it is believed to be difficult to reach these closed shells. In particular, it seems to be difficult to produce super-heavy elements near closed shells with sufficiently low excitation energy by means of stable beams (see figure 6). For example, the use of radioactive krypton isotopes will allow to produce new isotopes and maybe even new elements in the vicinity of the expected closed shells. The more neutron-rich super-heavy elements are not at all accessible with stable beams.

The identification of new super-heavy elements is usually based on the observation of their decay in a sequence of -decays. These -decay chains allow to link the new isotope to known lighter

super-heavy isotopes and thus to clearly identify the super-heavy nuclide produced. However, for the more neutron-rich super-heavy isotopes, these links to known isotopes do no longer exist, because the properties of the lighter decay products are not known. Therefore, it is of crucial importance to study the reaction mechanism to produce neutron-rich nuclei of elements between Z=100 and Z=110 as well as their decay properties. These isotopes can be produced with reasonable counting rates with neutron-rich fission fragments from SPIRAL2. The energies needed are around the Coulomb barrier.

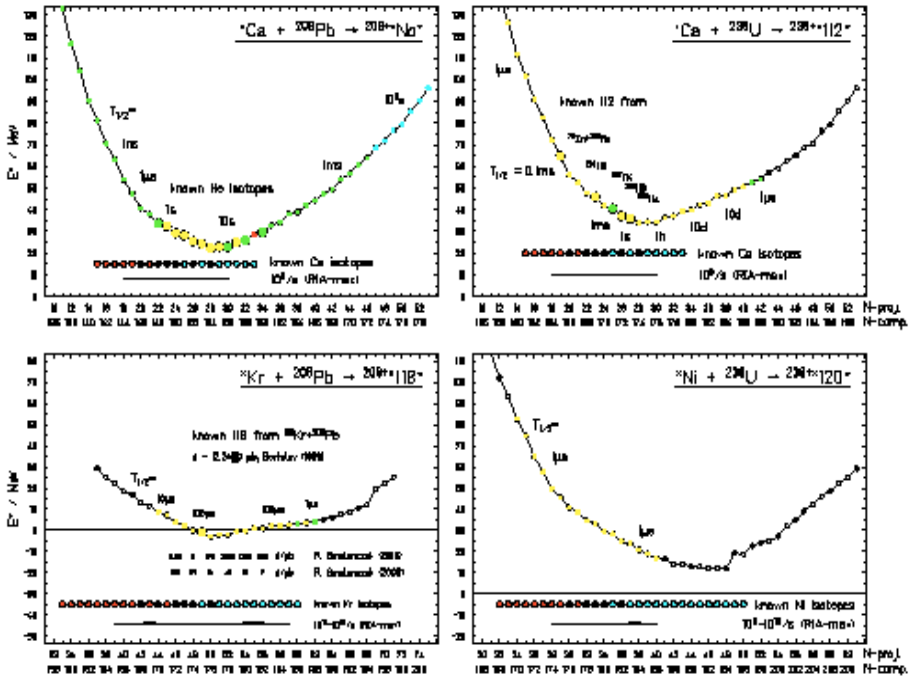

Figure 6: Excitation energy of compound nuclei for the production of super-heavy isotopes as a function of the isotopes produced with stable or radioactive beams. Shown are also the known isotopes for nobelium and element 112. The black circles are stable projectiles used for the production of the super-heavy isotopes. In red and blue are the radioactive isotopes used. In addition, predicted half-lives are shown. The bottom part indicates the stable (black dots) and known radioactive nuclei that can be used as they will be produced with high intensity. The x axis gives the neutron number of the projectile as well as of the compound nucleus (courtesy of S. Hofmann).

Nuclear astrophysics

To understand stellar evolution and the production of the elements in the universe, extensive model calculations are used to describe and simulate the different processes occurring in the stars.

Especially for violent processes like supernovae explosions or X-ray bursts, mainly properties of unstable nuclei are the most important inputs to the models. In neutron-rich stellar environments, the rapid-neutron-capture process produces heavy elements by a sequence of neutron captures and nuclear beta decays. To correctly model this r-process, the model inputs needed are masses of very neutron-rich nuclei, their beta-decay half-lives and their neutron-capture cross sections. However, up to now, these properties are only known for a few isotopes involved in the r process. Neutron-rich fission fragments from SPIRAL2 will allow to perform measurements of half-lives and masses for some of the key nuclei (see figure 7).

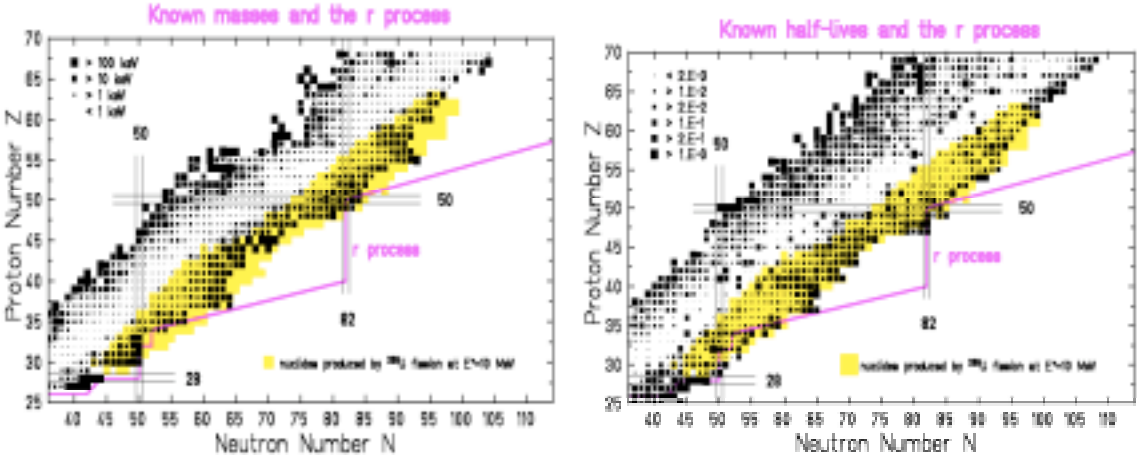

Figure 7: Left-hand side: Chart of nuclei of measured masses in the r-process region accessible with SPIRAL beams. The yellow part shows the region of nuclei produced by SPIRAL2 with photofission. In pink is indicated schematically the path of the r-process. The black squares indicate known masses where the size of the square is proportional to the uncertainty of the experimental mass. Right-hand side: Chart of known half-lives with the size of the squares proportional to their error-bars.

Neutron-capture cross sections are usually estimated by means of Hauser-Feshbach calculations. These calculations assume that a statistical picture is applicable for the capture process. However, close to magic numbers, and especially far from stability, the level density becomes so low that the statistical picture is no longer valid. Therefore, measurements are needed to determine these capture cross sections. A possibility is to measure cross-sections for neutron transfer via a (d,p) reaction with neutron-rich radioactive beams and to determine from these measurements the capture cross section for neutrons. This cross-section is known to be strongly influenced by the low lying strength of the giant dipole resonance and therefore coincidence measurements of fl rays are important as they provide information on the oscillation modes of the less bound neutrons. Regions of interest for these measurements are close to the magic shells at Z=28, N=50, and N=82.

Thermodynamics of the nucleus

In the following sections, we will address measurements that will be performed with a combination of stable and radioactive beams. They deal with thermodynamical properties of the atomic nucleus. Starting from less perturbative reactions, we will go to more and more violent collisions which pump more and more excitation energy into the nucleus.

Level densities and entropy

The level density is a basic ingredient of the nuclear equation of state. It allows to localize the opening of decay channels, to study correlation phenomena in the nucleonic movement, and to observe phase transitions. In addition, the level density is an important input for cross section calculations and its knowledge is essential for our understanding of astrophysical processes. At present, the level density has only been studied in nuclei close to the line of stability at low excitation energies. Recently, a new methodology has been proposed to measure level densities for stable nuclei. The measurements are based on particle-γ coincidences which allow to determine the level density for neutron-rich nuclei up to excitation energies of about 10 MeV. At the same time, phenomena like the quenching of pairing effects, the temperature dependence of the pygmy resonance, or the disappearance of shell effects can be studied. Using radioactive nuclei from SPIRAL2, these measurements will be extended to exotic neutron- rich nuclei around mass A=150.

Coulomb instabilities and limiting temperature

The limiting temperature a nucleus can stand is linked to a decrease of the level density at high excitation energies and its measurement helps to constrain the nuclear equation of state at finite temperatures in the vicinity of the saturation density. For stable nuclei, the limiting temperatures are rather high and, to investigate this parameter, one needs to control the energy deposited, the degree of equilibration, and the reaction mechanism.

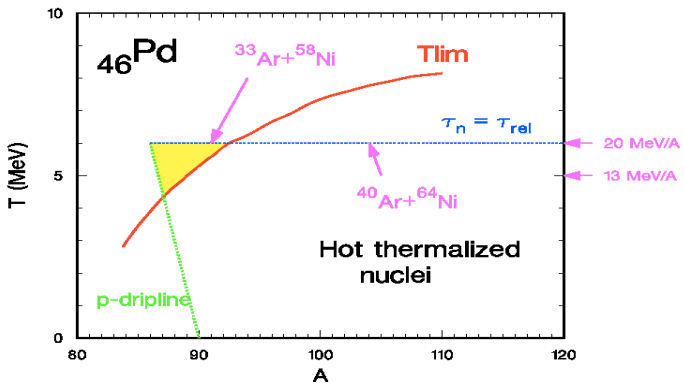

Figure 8: The limiting temperature is plotted on a graph of the temperature versus the mass of the compound system. By changing the incident energy and the projectile/target combination from a proton-rich to a neutron-rich combination, different regions below and above the limiting temperature can be reached.

In the vicinity of the proton drip line, Coulomb instabilities are predicted to decrease drastically the limiting temperature (see figure 8). The proposal is to study an isotopic chain of compound nuclei

produced via fusion-evaporation reactions from the proton-rich side (SPIRAL1) to the neutron-rich side (SPIRAL2) by precisely measuring the deexcitation pattern of particle emission in coincidence with evaporation residues in an excitation energy range between 1 MeV/nucleon and 3 MeV/nucleon. Additionally, these studies allow to investigate the influence of the Coulomb interaction on the expansion of a nuclear system initially strongly compressed.
These studies require projectiles of e.g. ^{114}Xe to ^{145}Xe at energies of 5 MeV/nucleon to 30 MeV/nucleon with intensities of about 10^6 particles per second impinging on calcium targets. Other systems to be studied are based on beams of $^{74\text{-}96}$Kr impinging on iron targets.

Reaction mechanism and thermodynamical equilibrium

The degree of thermal equilibration of a nuclear system can be studied as a function of the deposited energy by detecting particles emitted in the reaction. These studies, performed over wide ranges of isospin, provide information necessary for investigations of the thermodynamics of nuclear systems at high excitation energies in order to identify an equilibrated source of particle emission and thus to control the reaction mechanism.
Using projectile/target combinations with different isospin, the mapping of the N/Z ratio of light particles as a function of the rapidity allows then to determine the degree of equilibration of a nuclear system.
This technique has been employed in experiments at the FOPI detector of GSI, where a large part of the energy available is collective. At lower incident energy, a large part of this energy should be available to thermalize the system. In order to perform this kind of studies, a detector capable to identify fragments in A and Z is necessary. As the degree of equilibration depends on the mass of the system, light and heavy systems have to be investigated. Some of the systems (e.g. $^{83\text{-}106}$Nb on ^{54,58}Fe or $^{114\text{-}145}$Xe on ^{112,124}Sn) can be studied at SPIRAL1 and SPIRAL2.

Transport properties and symmetry energies

Sophisticated transport models predict large-amplitude fluctuations of the matter density and of the isospin content in the interaction region of binary collisions at the Fermi energy.
These fluctuations can be observed by measuring isotopic distributions of fragments at mid-rapidity between the quasi-projectile and the quasi-target. A comparison to theory allows to link the distribution to the dissipation properties of the nuclear transport and to the density dependence of the symmetry coefficient of the equation of state of asymmetric nuclear matter. To control the reaction mechanism and the degree of dissipation, it is necessary to detect coincidences between the quasi-projectile and the intermediate mass fragments which have to be identified in mass and charge. These studies can be performed with similar beams as those mentioned in the previous paragraph.

Multifragmentation and the liquid-gas phase transition

The observation of a negative heat capacity via the measurement of fluctuation in the reaction Q value has allowed recently to demonstrate that multifragmentation corresponds to a liquid-gas phase transition. The same analysis performed with exotic nuclei will allow to study the phase diagram as a function of isospin. The observation of fossile signals of the spinodal decomposition in the charge correlations between fragments suggests that the phase transition is driven by density fluctuations amplified by the mechanical instabilities of the spinodal region.

Theory predicts that, for neutron-rich systems, the phase transition is due to a chemical spinodal zone which leads to a fractionation of isospin: the heavy fragments are more proton rich, whereas the lighter fragments are neutron rich. Again, an unambigous determination of the fragments in A and Z is crucial to perform these kinds of studies. Incident energies of the order of 30 MeV/nucleon are necessary to reach the threshold for multi-fragmentation. It is of interest to study exotic isotopes of the same systems for which the phase transition has been observed. Therefore, beams of $^{114\text{-}145}$ Xe on tin targets as well as gold-on-gold reactions ($^{176\text{-}205}$ Au + ^{197}Au) are required.

Summary

The subjects mentioned here represent only a few selected topics of nuclear physics interests that can be addressed using beams of neutron-rich fission fragments. The presented cases show that a wide variety of problems in nuclear physics and nuclear astrophysics can thus be addressed. Therefore, low- and medium-energy beams from SPIRAL2 up to some 50 MeV/A will open new exciting possibilities in different fields of nuclear physics and applied nuclear physics.

Production of heavy neutron-rich beams

Fast neutron induced fission

The aim of the SPIRAL-II project is to establish the feasibility of producing accelerated beams of neutron-rich radioactive beams with the existing radioactive beam facility SPIRAL at GANIL. The neutron-rich radioactive nuclides are to be produced by fissioning a heavy nuclide, such as ^{238}U. The technique originally proposed for SPIRAL-II is the use of energetic neutrons to induce fission of depleted uranium. The neutrons are generated by the break-up of deuterons in a thick target, the so called converter, of sufficient thickness to prevent charged-particles to escape. The energetic forward-going neutrons impinge on a thick production target of fissionable material. The resulting fission products accumulate in the target, diffuse to the surface from which they evaporate, are ionised, mass-selected and finally post-accelerated. This method has several advantages. The highly activated converter can be kept at low temperature without affecting the neutron flux. The target is bombarded by neutral projectiles losing energy only by useful nuclear interactions and having a high penetrating power allowing very thick targets.

One of the main objectives of the R&D program (for details see ref [1]) was to determine the intensity and energy of the primary deuteron beam giving the best yields of radioactive nuclides of interest for radioactive beams while taking into account beam power evacuation and safe operation of the facility. The approach has consisted in carrying out simulations with various codes available or developed by our different task groups and performing a number of key experiments to validate the simulations. In this way, confidence is gained about the predictive power of the codes for situations where experiments could not be set up within the allocated time for the study.
The concept of using neutrons generated by deuteron break-up implies a study of production yields, energy spectrum and angular distributions of neutrons in converters made of various materials and as a function of deuteron energy. Experiments were performed at IPN-Orsay, KVI-Groningen and Saturne at Saclay. They explored a range between 14 and 200 MeV deuteron energy. The main features of neutron spectra are listed below

At forward angles, the energy distribution has a broad peak centred at about 0.4 times the deuteron energy. The angle of emission becomes narrower with increasing energy. For 100 MeV deuterons, the energy width (FWHM) of the neutron spectrum is about 30 MeV and the FWHM opening angle of the cone of emission is about 10 degrees.

There is a rather isotropic distribution of neutrons of a few MeV due to evaporation in fusion reaction.

The angular distributions and energy spectra are in fair agreement with calculations with an extended version of the Serber model and with the LAHET code. The Serber model reproduces the distributions of high-energy neutrons but not of the low-energy neutrons since evaporation is not

implemented in the code. LAHET reproduces the low energy neutron spectrum while it tends to slightly underestimate (less than a factor 2) the neutron distributions at very forward angles.

A strong increase in neutron production is observed between 14 and 100 MeV deuteron energy. It is much less pronounced between 100 and 200 MeV. Among converters tested Be is slightly more productive than C. It has, however, disadvantages related to its physical and chemical properties.

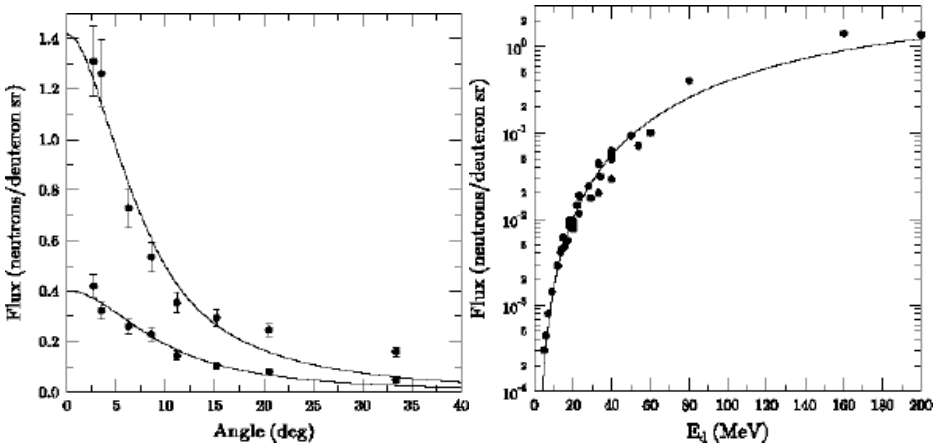

Experimental angular distributions of neutrons for 80 and 160 MeV deuterons incident on a thick Be target (left). Neutron yield at 0° as a function of the incident deuteron energy for a Be converter(right).

Cross sections for n-rich nuclei in neutron-induced fission

Another step is the measurement of fission cross sections for n-rich nuclei at intermediate neutron energies. Magnitudes and widths of distributions for neutrons of average energy 20 MeV generated by the 50 MeV deuteron beam on a ^{238}U target are similar to those obtained with 25 MeV protons. Yet, for a given element, they are shifted towards larger mass by about 2 mass units. In that respect, they are similar to the distributions by thermal n-induced fission on ^{235}U. However, fast neutrons produce a much wider distribution with higher cross sections at very asymmetric mass splits (A=80,160) and in addition, the dip in the symmetric region (A=120) is almost filled. These results have been used to extend a model originally designed for fission induced by intermediate energy protons.

Comparison with data for 2.5 MeV neutrons shows that about 1.4 neutron is lost when the neutron energy is increased from 2.5 MeV to an average of 20 MeV. Due to increased excitation energy of the compound nucleus, high energy favours production of less n-rich fragments. On the other hand, the total fission cross section increases up to about 40 MeV neutron energy and neutron production further increases. This implies the existence of a certain optimum for producing neutron rich nuclei.

Studies with a system formed with converter and target

It is also necessary to consider the geometry of the converter + target assembly. The target must intercept a large fraction of the neutrons. Thus, it must be close enough to the converter to subtend

a high solid angle. The target temperature must be high enough to allow fast and efficient release of the fission products. These studies have been performed with devices designed and constructed at the IPN-Orsay referred as PARRNe1 and PARRNe2 [2]. They both include a converter and a target. Various materials for the converter and two different targets, a high temperature porous UCx and a liquid uranium target, have been tested.

In a recent experiment at PARRNE2 with the fast release UCx target (December 2000) a MK5 plasma source similar to the one at CERN-ISOLDE has been used. PARRNE2 indeed is able to deliver most of the elements available at ISOLDE. Among the very encouraging results is the separation of the double magic ^{132}Sn produced, extracted from the target, singly 1^+ ionised and mass separated with a rate of 3.5 10^5 / s. Extrapolation (from measurements done at different energies on noble gases) at 100 MeV and 500 µAe let expect for 1.7 10^9 single-charged ions / s of ^{132}Sn delivered for charge breeding and post acceleration. The rates for elements extracted and ionised as singly charged 1^+ ions are shown on the figure below.

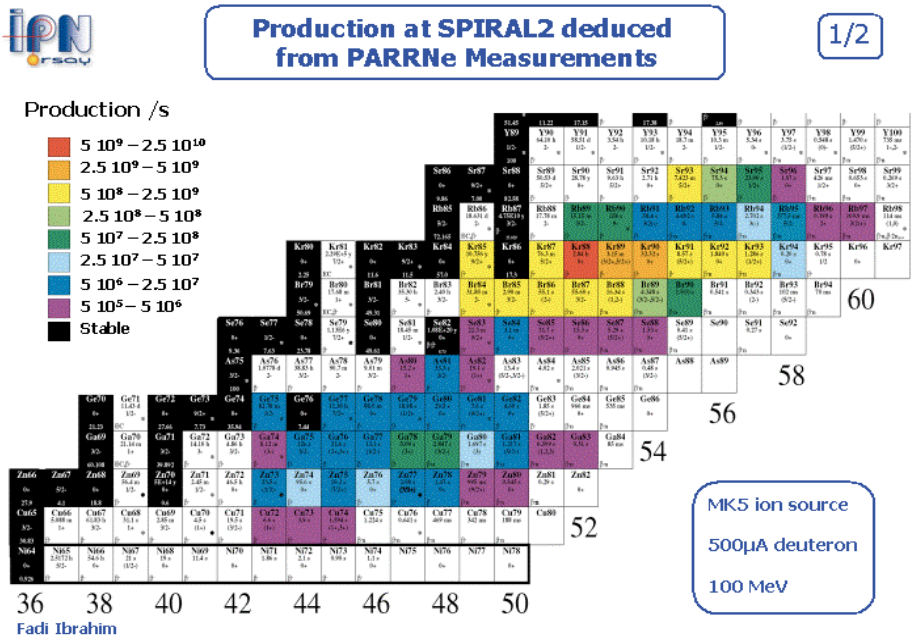

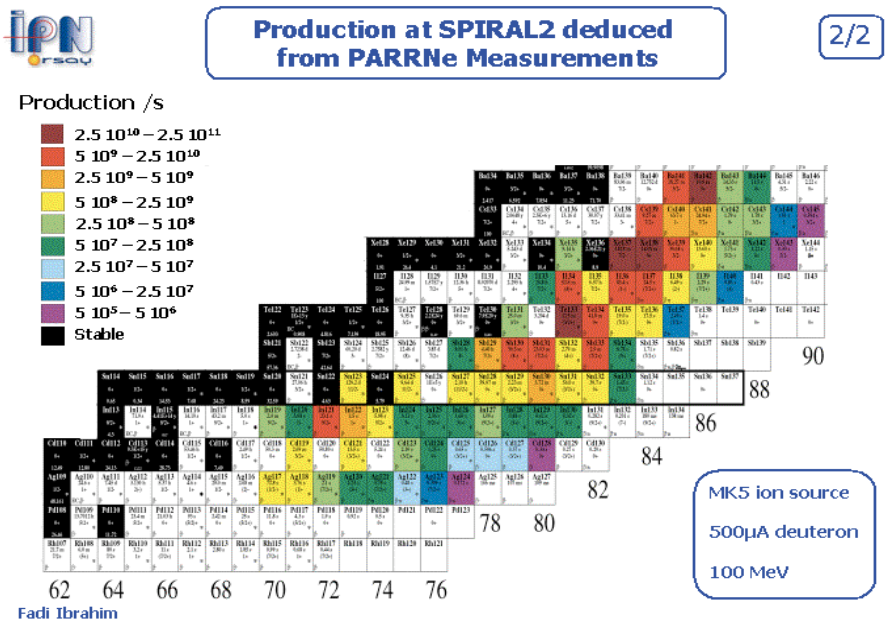

Diffusion depends critically on the structure of the target material and on the temperature. At IPN-Orsay, R&D has been devoted to UCx targets following the technique elaborated at ISOLDE and to molten uranium targets. The UCx and molten target are complementary. The higher temperature and shorter path to the surface in the grains of the porous UCx target favour fast diffusion ($T_{release}$ = 5 s for Xe). The molten uranium target has a larger amount of uranium but slower release ($T_{release}$= 112 s for Xe). The former is more efficient for short-lived activities, while the latter is more suited for longer-lived activities up to half-lives of 30s. Further research is needed in order to find the optimum material structure, such as composition and density, for the targets and coupling to the ion source. These properties play a major role in the diffusion and thermal behaviour of the target.

According to several experimental observations the deuteron energy of 100MeV is near the best value. In short, this results from the energy dependence of neutron yield, neutron energy spectrum and angular distribution the energy dependence of total fission cross section, which reaches a maximum at 40 MeV neutron energy (i.e. 100 MeV deuteron) and the energy dependence of nuclide cross-sections. For a fixed number of total fission, nuclei of asymmetric region are similarly produced at lower energy while the others at higher energy. An energy around 100 MeV appears to be a good compromise.
The LAHET and FICNeR codes also show that the number of fissions per kW of accelerated deuteron beam first strongly increases with energy but near 100 MeV saturates.

Power load on target and beam intensity limit
The maximum beam intensity which can be withstood by the converter or target define the maximum production rates achievable at the best deuteron energy:
The converter can accept a beam intensity of 350 µAe at 100 MeV if the beam is defocalised to a 2 cm radius. The limit is actually due to cooling of the outer surface of the C-converter. With a higher

heat exchange coefficient (but within a factor of 2 higher) than presently the GANIL standard, it should be possible to accept 500 μAe on the converter. An alternative solution would be a fast rotating converter.
The conventional method is to let the beam to impinge directly on the target. In this case, it is better to let the beam to exit the target. This avoids unnecessary heating by the ions close to the end of their range (the Bragg peak). Nevertheless, only a 50 μAe beam of 2 cm radius is possible on this target. The major drawback is certainly the lack of temperature control else than via the beam intensity.

Yields have been obtained with the LAHET+MCNP+CINDER code for radioactive beam intensities consistent with temperatures which the target can stand and an energy of 100 MeV. The 350 μAe beam on the converter induces 6 10^{12} fissions / s in the target while this is 1.2 10^{13} without converter with 50 μAe beam. However, yields of the most neutron-rich nuclei are higher with the converter, owing to the lower projectile energy (neutrons of 40 MeV average energy) and the formation of a more n-rich compound nucleus (no proton is captured).

Ionisation
The atoms diffused out of the thick target must be ionised. The most recent PARRNe2 experiment, with a MK5 plasma source designed at ISOLDE, was promising. However, depending on the element to be ionised it is necessary to use several sources to guarantee for highest efficiency and/or selectivity. So far considered are a ECR-source for gases and volatile elements, e.g. MONO1001 at GANIL, a surface ionisation source for alkaline and earth-alkaline elements and a more universal plasma source with hot transfer line, e.g. the ISOLDE MK5 source. These sources could have efficiencies close to 100% for rare gases and alkalines, and between 10% and 50% for other elements. Moreover, a laser ion-source is well suited for specific cases where especially high purity is compulsory.

Charge breeding is necessary in order to accelerate the ions to final energies above the Coulomb barriers. Typically, the charge state must be increased up to at least one third of Z. Efficiencies are presently between 3% and 12% for the most probable charge, depending on the elements.

Safety considerations
There is, to date, no facility comparable to the design goals of SPIRAL-II. Therefore, radiation doses and production of contaminants have been estimated by using the LAHET-MCNP-CINDER code at GANIL. This has been carried out for different configurations, converter material and deuteron energies. Considering the radiation doses (proportional to the beam intensity) for the same production of nuclei of interest, we arrived to the following conclusions:
Alpha-activities one year after the beam stopping are produced in large amounts at the highest energies since reaction channels for actinides is opened for more nuclei at higher energy. The □-

activity is higher for deuteron beam on a UCx target in the direct method than with a converter. Tritium production is larger with light-Z converters (C, Be or Li) than without. Carbon is the lowest producer of tritium among them.

For a fixed number of fission/s, the radiation doses during operation and most residual activities after a long term shut down are weakly depending on the energy. The only exception is for tritium production, which increases monotonically by a factor of 9 between 50 MeV and 200 MeV. Nevertheless, this increase is a factor of 2.5 from 50 MeV to 100 MeV. Production of alpha-activities is clearly the lowest near 100 MeV. In conclusion, the energy of the deuteron beam for safe operation, taking into account the production of β emitters, is 80-100MeV. This is the same range as it was determined to be best for production of neutron-rich nuclides.
Moreover measurements have been performed. The attenuation length of neutrons in concrete has been measured at GANIL in order to better estimate the amount of concrete shielding for neutrons needed during irradiation. Activation of air in the target area has been measured at Louvain-La-Neuve to validate the safety codes. Finally, a method has been developed and tested in order to measure the amount of tritium escaping from the target by diffusion.

Photofission

It has recently appeared that photofission could be an alternative to n-induced fission. This working group has therefore initiated a study of photofission induced by Bremsstrahlung generated by electrons. The respective merits and technological challenges of these two methods will be evaluated in order to made the best choice for SPIRAL-II.

With an electron driver, electron interaction with matter will radiate Bremsstrahlung photons inside the target. Fission will then be induced by those photons exciting the Giant Dipolar Resonance (GDR) of the nucleus at the right energy. This well-known process is called photofission.
The GDR cross section for ^{238}U is shown in the figure below on the left. A maximum fission probability of 160 mb is obtained for photons having energy around 15 MeV. At that energy, the photoelectric and the Compton and Rayleigh scattering cross sections are starting to fall off rapidly so the main contributions to gamma absorption are e^+e^- pair production and the photonuclear reactions (γ,*f*), (γ,n) and (γ,2n). Although the absolute fission cross section is rather small (compared to normal fission with neutrons), its contribution is not negligible as even a pair production reaction may in a thick target eventually lead to a fission through the resulting photon produced. In the same manner the neutrons produced by (γ,n) and (γ,2n) reactions as well as the (γ,*f*) itself can also induce fission, this time by the regular (n,*f*) high cross section (0.5 barn for fast neutrons). Therefore, in a thick target, photofission may be a rather interesting way of creating radioactive fission fragments.

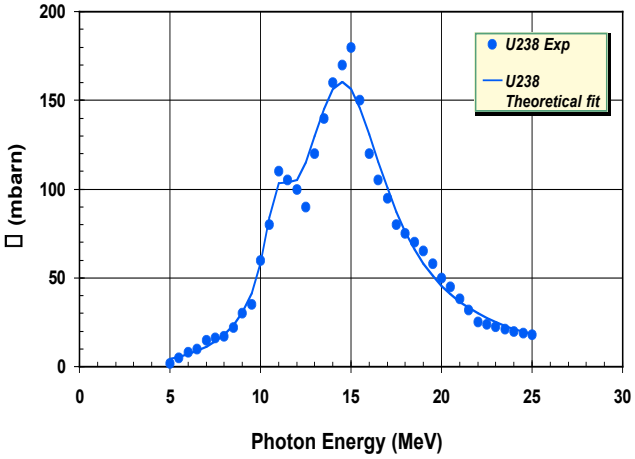

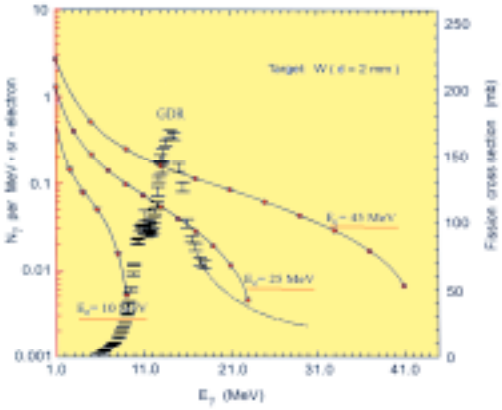

Photofission cross-section for ^{238}U above (left and right) and rate of fission per electron according to incident energy of the electrons (right).

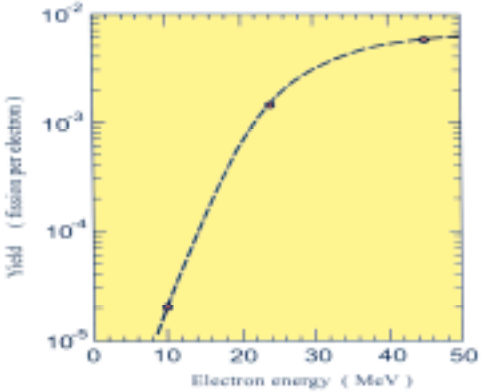

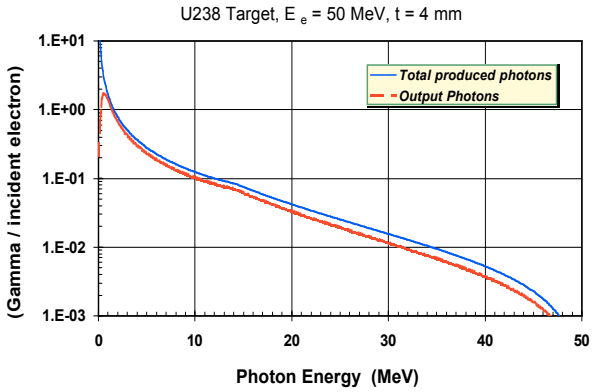

Photon energy distribution by Bremsstrahlung in ^{238}U

Unfortunately, no efficient monochromatic sources of 15 MeV photons are available. The most common way for producing high gamma fluxes is the Bremsstrahlung radiated by passage of electrons through matter. This process has a cross section rising linearly with energy. It will dominate the ionization process above a critical energy (around 20 MeV). But the resulting Bremsstrahlung spectrum is widely spread in energy from zero up to the full initial electron energy (figure above). Although each single electron may ultimately produce as high as 20 photons, only a small fraction of it (0.5 to 0.7 gamma per e^-) are "useful" photons lying in the GDR range (15 ±5MeV).

A simple calculation including the main electron interactions (Bremsstrahlung and ionization) and the main nuclear reactions of interest (pair production and fission cross section) in a thick depleted uranium target can give the expected number of fission per incident electron. In the figure below, the number of fissions produced by the (γ,*f*) reaction is plotted as a function of the electron energy. This result is a complete Monte Carlo calculation performed with a MCNP code offering also photonuclear capability (full electron, photon and neutron transport). The obtained result is in accordance with the simple analytic calculations. For comparison, fission production is also given when using a tungsten converter (5 mm thick) in front of the ^{238}U target. It appears that when using a converter in the electron driver option, less than 30% of the beam power is lost inside the converter (in contrast to the d driver option). In the direct method one will produce about 25% more fission per electron (and probably more when taking in account neutron induced fission). Fission production is almost linear above a threshold energy of 10 MeV. High production is obtained above 40 MeV.

As the SPIRAL II project is aiming at 10^{13} fissions/s, the required beam intensity should be 500 μA for an electron energy of 45 MeV directly on the target.

In order to compare rapid neutron induced fission and photofission, measurements of Kr and Xe isotopic distributions produced by photofission and diffused out of a thick UCx target has been performed using the same PARRNe1 device in the same conditions that with deuterons beams and with the same target. The measurements have been done with a 4 mm W converter in different

position (8 mm from the target, 4 mm from the target) and one measurement without W converter. Comparison with the 80 MeV deuteron induced fission measurements are presented below.

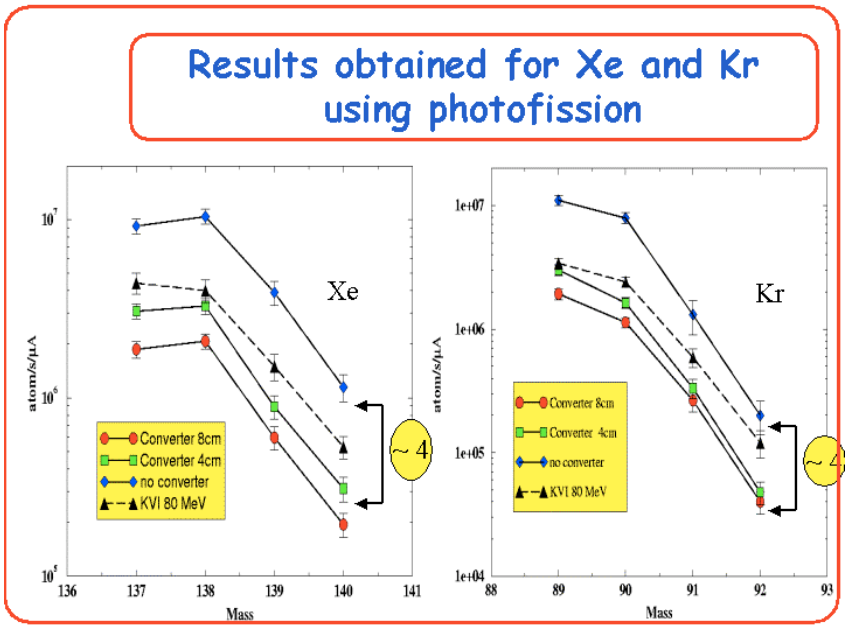

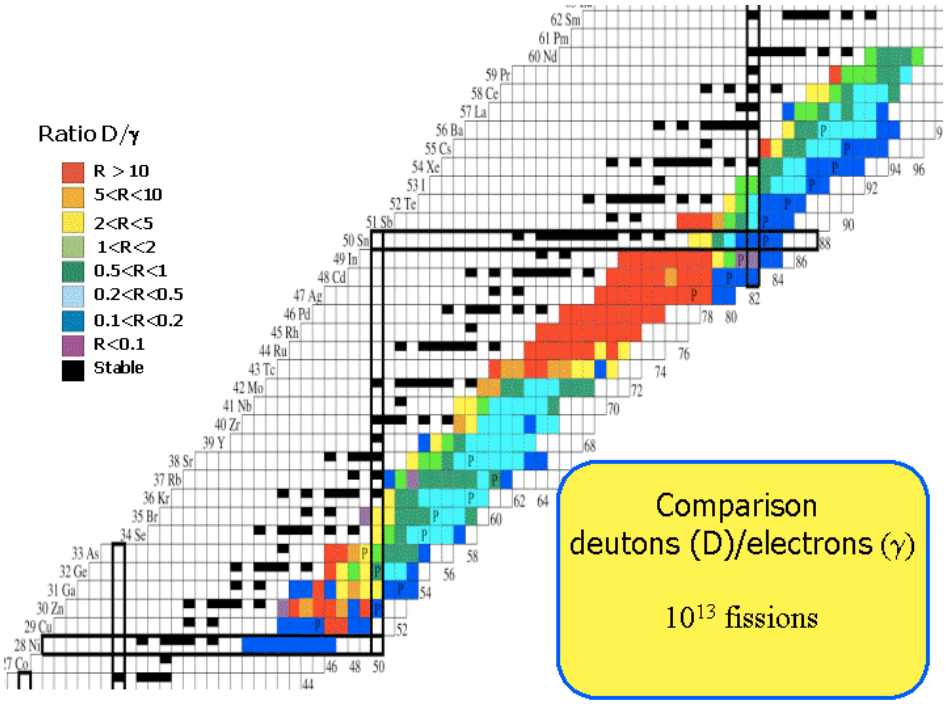

The results obtained are well understood taking into account the percentage of photons between 11 and 17 MeV emitted in the cone subtended by the target that is the solid angle.

Finally, the above figure summarizes some comparison of production yields normalized to 10^{13} fissions for 100 MeV deuterons (LAHET calculations) and 50 MeV electrons based of the K-H Schmidt estimations.

In the case of the electron driver, much work remains to be done in the design of the converter and of the UCx target specially to resolve problems related to the beam power dissipation in the target. **This work is still in progress and constitute one major point of the success of induced photofission with an electron beam.**

The deuteron driver for the SPIRAL-II project

Three options for the accelerator providing the deuteron beam for the neutron production in the SPIRAL-II project have been studied

- the actual GANIL cyclotrons
- the SARA booster-cyclotron with a new injector
- a new cyclotron.

In the present chapter the specifications of the deuteron accelerator and the different options for such an accelerator at GANIL are discussed.

Accelerator type

From a technical point-of-view both a cyclotron and a linear accelerator are suitable to produce the 80 MeV deuteron beam needed. For cyclotrons the presently achieved maximum beam intensities are about 1 mA of 30 MeV protons in commercial compact cyclotrons used for isotope production and 2 mA of 72 (and 590) MeV protons in the separated sector cyclotrons at PSI (Switzerland).
For linear accelerators the achievable currents are significantly higher. However, at the low energy (80 MeV) needed for the present application and assuming that the required intensity can be provided by a cyclotron linear accelerators are much less cost-effective. They have a larger footprint, thus requiring a higher investment for infrastructure (building etc.), while also the accelerator itself is far more expensive than the equivalent cyclotron. Finally, if CW operation is required only a linear accelerator with superconducting RF cavities can be used, which further increases the investment.
It is concluded that for the SPIRAL-II project the use of a cyclotron is the best option: it permits to achieve the objectives of the project at the lowest costs. However, as a consequence of this choice, a significant increase in intensity in the framework of a future upgrade will require large additional investments.

Cyclotron characteristics

Radiation safety is a very important issue when accelerating deuterons to an energy of 80 MeV with an intensity up to 0.5 mA. Beam losses around 1 % already cause strong activation of the parts of the cyclotron on which the lost beam impinges. Furthermore a large flux of high energy neutrons is produced, which will significantly activate the cyclotron and its surroundings. This flux of neutrons is increased even further because of the low threshold for neutron production in the

$d(d,n)^3He$ reaction on lost deuterons that have been implanted in various parts of the cyclotron. Furthermore tritium is produced via the reaction $d(d,p)^3H$. This may lead to additional radiation safety problems.
It is thus essential that a very high transmission (≥ 99.9 %) is achieved, in particular for the later stage of acceleration and for the extraction. It is the prime factor in assessing the suitability of the three possible systems studied:

The actual GANIL cyclotrons

The actual GANIL cyclotrons can accelerate deuterons to energies in the range from 12 to 26 MeV and probably around 80 MeV. With the injector cyclotron and the first separated sector cyclotron the energy range 12 to 26 MeV can covered without modifications of the accelerators. The fission yield at 26 MeV is at least an order of magnitude lower than at 80 MeV, taking into consideration the energy dependence of the neutron production and fission cross sections.
Around 80 MeV it seems possible to accelerate deuterons using the complete chain of injector cyclotron and two separated sector cyclotrons. In the injector cyclotron and the first separated sector cyclotron molecular ions would be accelerated, which would be stripped into two deuterons on injection in the second separated sector cyclotron. As the neutron production by deuterons at this energy is at least an order of magnitude higher, radiation safety problems will impose much more serious constraints, connected to both the shielding and the activation of components.
The feasibility of 80 MeV deuteron beams as well as the radiation safety and technical constraints on the beam intensity are subject to further study.

The SARA booster-cyclotron with a new injector

The SARA booster-cyclotron is a separated sector cyclotron, which is presently being decommissioned at the Institut des Sciences Nucléaires in Grenoble (France). It can accelerate deuterons to a maximum energy of 72 MeV, slightly lower than the value aimed at. It has an energy gain of a factor 5, so that an injector (cyclotron) delivering 14.5 MeV deuterons is needed. The matching conditions between the injector and booster cyclotron strongly constrain the characteristics of the injector. Consequently the injector will have to be specifically developped. Furthermore the injection, RF-system and extraction of the booster will have to be reconstructed to meet the requirements of the high intensity operation.
The requirements on the extraction efficiency can only be met by the use of stripping extraction of negative ions. These negative ions thus have to be extracted from the injector by a standard extraction system using an electrostatic deflector. Taking into consideration the lower yield and energy of neutrons produced at 14.5 MeV as compared to 80 MeV the extraction efficiency of the injector should be at least 95 %, which is close to the limit of feasibility.

A new cyclotron

An analysis of the existing cyclotrons delivering high intensity proton beams (≥ 1 mA) at a fixed energy shows two possible schemes to achieve the required transmission:
A large, low-field separated sector cyclotron with high energy gain per turn and 'classical' extraction (*e.g.* PSI injector II: 2mA 72 MeV protons). Cyclotrons of this type have been developped

exclusively for research institutions. The high transmission is obtained by maximizing the radial distance between subsequent turns in the machine, so that an electrostatic septum, which bends away the last turn, can be inserted inbetween two turns.
A cyclotron for 80 MeV deuterons based on this approach would have an extraction radius of 3.5 m.
A compact cyclotron accelerating negative ions with stripping extraction (*e.g.* IBA (Belgium) CYCLONE30 and EBBCO (Canada): TR30, both delivering 1 mA 30 MeV protons). Around 20 cyclotrons of this type are used routinely for isotope production in an industrial environment. The efficiency of the extraction process is about 100 %; the overall transmission is determined by beam losses during acceleration caused by the magnetic field and the interaction with the residual gas.
A cyclotron based on these examples would have an extraction radius of about 1.6 m. For the present application the superior beam quality of the first, far more expensive scheme is not required. Furthermore, the use of stripping extraction makes it possible to vary the energy over a range of roughly a factor two (40 – 80 MeV) by changing the radius at which the stripper foil is located.

Analysis and recommendation
The use of the present GANIL-cyclotrons requires by far the lowest investment. The investment for a dedicated accelerator (compact cyclotron or SARA booster + injector) is estimated to be of the same order of magnitude (10 – 12 MEuro excluding infrastructure).

The installation of a dedicated accelerator will make the operation of the SPIRAL-facility (and of the GANIL-facility in general) more flexible, efficient and versatile:

- development work on beams with SPIRAL-II can proceed while beams from SPIRAL-I or the present GANIL-facility are delivered for experiments.
- operation of the SPIRAL-facility is decoupled from that of the present GANIL-cyclotrons.
- the intensity of the radioactive beams attainable is at least an order of magnitude higher, thus significantly extending the range of feasible experiments.
- the possibility to inject beams from SPIRAL-II into the present GANIL-cyclotrons remains open.

Simplicity of both concept and operation is an important asset for the deuteron accelerator in the SPIRAL-II project. The compact cyclotron accelerating negative ions has by far the best score on this aspect.
The development and construction connected to the use of the present GANIL-cyclotrons or the SARA-booster will require a large effort from the accelerator staff of GANIL (or other possible partners in the project). The development and construction of the compact cyclotron, based on existing industrial designs, is suitable for contracting to industry.
It is thus concluded that a dedicated compact cyclotron accelerating negative ions is the optimal solution for the deuteron option for a short term in the SPIRAL phase II -project.

The Electron Driver Accelerator for SPIRAL II

General Layout

The accelerator layout is shown below and is quite similar to the MACSE project [3] The injector comprises a 100 keV gun and a short cryomodule containing a single superconducting cavity. At the injector exit, the electron beam is already well relativistic. Then the beam runs in a long cryomodule through four SCRF cavities bringing the electrons to the final energy of approximately 45 MeV. A bending magnet followed by a transport beam line will get the beam at the right place and shape onto the target.

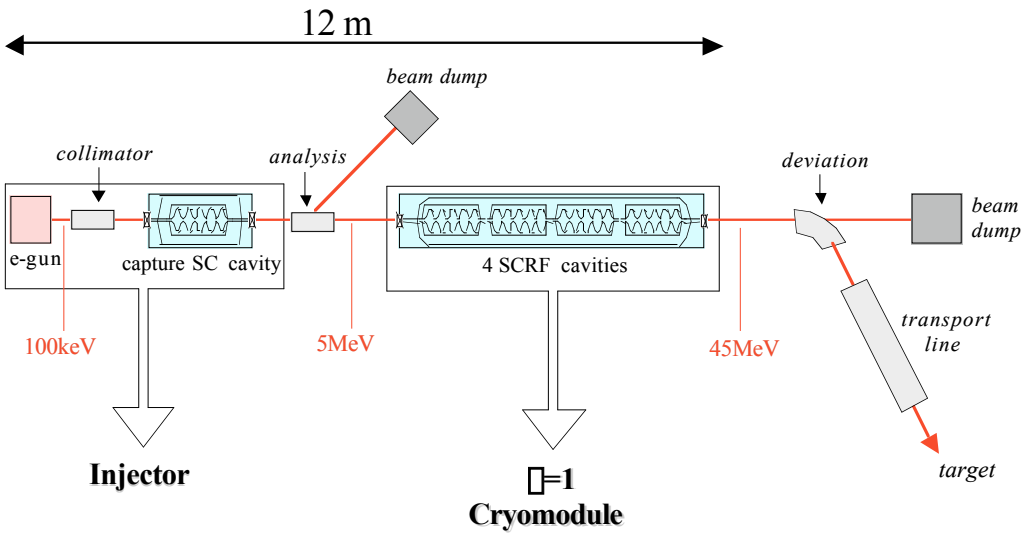

Layout of the electron driver.

Gun

The gun uses a standard thermoionic cathode sited on a 100 kV platform. The power supply can deliver up to 3 mA in current. In order to bunch the beam at the proper frequency of 1.5 GHz, a specific line consisting of two rectangular RF cavities (chopper) are used to cut a 60° phase out of the DC beam delivered from the cathode. Another cylindrical cavity (buncher) is used to bunch the beam down to a 10° phase at the entrance of the capture cavity.

An attractive alternative method would be to set up a gridded cathode similar to the one used in Inductive Output Tubes (IOT). In that way, the beam could be bunched right from the starting emission point that suppresses the need of the rather cumbersome bunching line. This new technique will be tested at CEA/Saclay in 2001 and if successful, will be implemented on the SPIRAL II machine.

A collimator can be placed after the gun in order to control the beam emittance. This could be of importance for safety and radiation issues (see below) as undesired beam tails can be quite easily suppressed at that stage without creating too much radiation.

Capture Cavity

The capture cavity is a superconducting cavity with a reduced beta value due to the not fully relativistic beam coming out from the gun. Geometry has to be optimized to properly capture the beam without degrading too much the longitudinal emittance. The figure below shows some simulations where different cavity shapes have been studied.

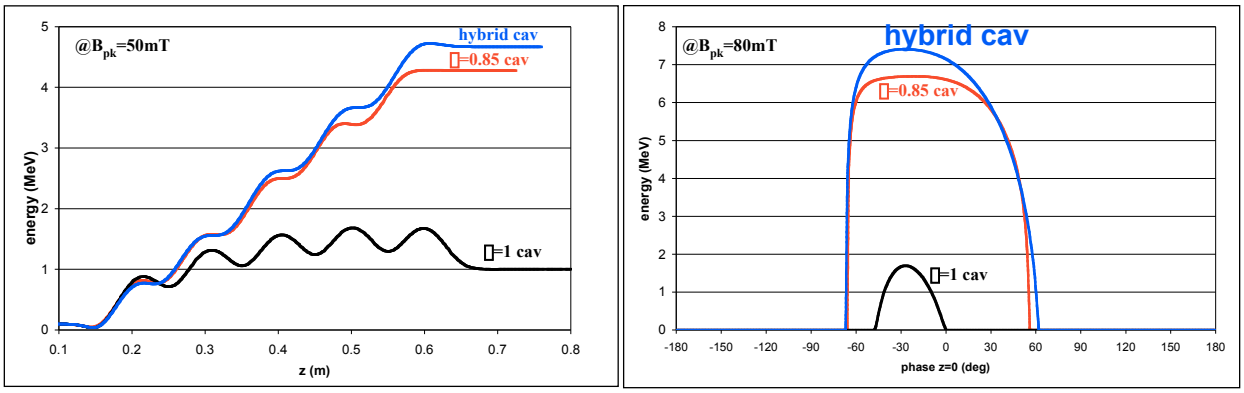

Output energy as a function of position and phase for three different cavity shapes. A β = 1 cavity is clearly not adequate to use as a capture cavity.

The output dispersion of the beam shown on the figure below is simulated for two different cavity shapes assuming an input beam with 200 eV and 30° extension in phase. It can be noticed that the output beam will feature less than 40 keV and 5° in the longitudinal phase space.

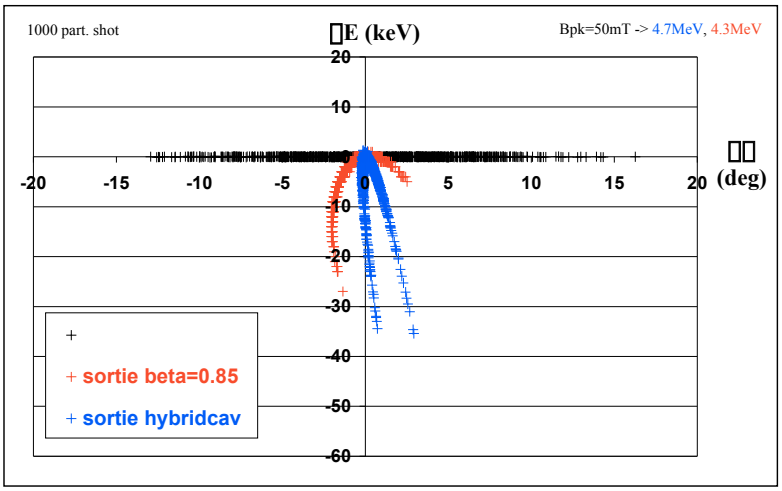

Longitudinal dispersion at the output of the capture cavity for two different shapes.

SCRF Cavities

The four SCRF cavities are standard β=1 elliptical cavities working at the resonance frequency of 1.5 GHz. The characteristics of these cavities are summarized in Table I. The important thing to point out is the high accelerating field operation (19 MV/m) and the very low bandwidth (40 Hz) due to the low beam current.

The cavity will use an integrated helium tank vessel and a specific tuner will have to be developed. A great care should be taken as regard to the low bandwidth. Therefore, any improvement made on tuners developed in the frame of the CEA/Saclay-IPN/Orsay collaboration for SCRF cavities could be implemented in SPIRAL II. For example, the use of piezoelectric tuners if demonstrated would be of great benefit.

SPIRAL II SCRF CAVITY						
Frequency	1 500.000000	MHz		Beam Power	4.756	kW
□	1.000			Dissipated Power	9.058	W
□	0.200	m		Incident Power	4.767	kW
(□□□/2)	0.100	m		Incident Q	3.80E+07	
(r/Q)/cell	50	□		Zero Current Voltage	1.90E+07	V
				Slope X	1.90E+10	□
Number of cells	5			V	9.52E+06	V
Bpeak	80	(mT)				
Bpk / Eacc	4.2					
Eacc	19.05	(MV/m)				
Q0	2.00E+10			All External Q's	1.00E+11	
Length	0.500	m		Loaded Q	3.79E+07	
(R/Q)	250	□		Bandwidth (2.□f)	40	Hz
Stored Energy	19.222	J		β_{inc}	0.997724	
				β_{cavity}	0.001897	
Maximum Voltage	9.52E+06	V		β_{ext}	0.000379	
Beam Current	5.00E-04	A				
Phase	2.000	degrees		Reflected Power	1.72E-04	W
Actual Voltage	9.51E+06	V		Cavity Losses	9.058	W
Energy Gain	9.512	MeV		Transmitted Power	1.812	W
Detuning Angle	-1.992	degrees				
Cavity Frequency	1 500.000	MHz				
Frequency Shift	-0.69	Hz				

Table I – Typical SCRF cavity characteristics.

Cryomodules

Two separate cryomodules are needed. The first will house the single capture cavity and the second one the four SCRF □=1 cavities. These cryomodules are similar to the one used on the MACSE test bed but will be modified to take in account the fact that the helium vessel is suppressed, each cavity having an individual helium tank. Schematic drawings of the largest cryomodule are shown in the next figures.

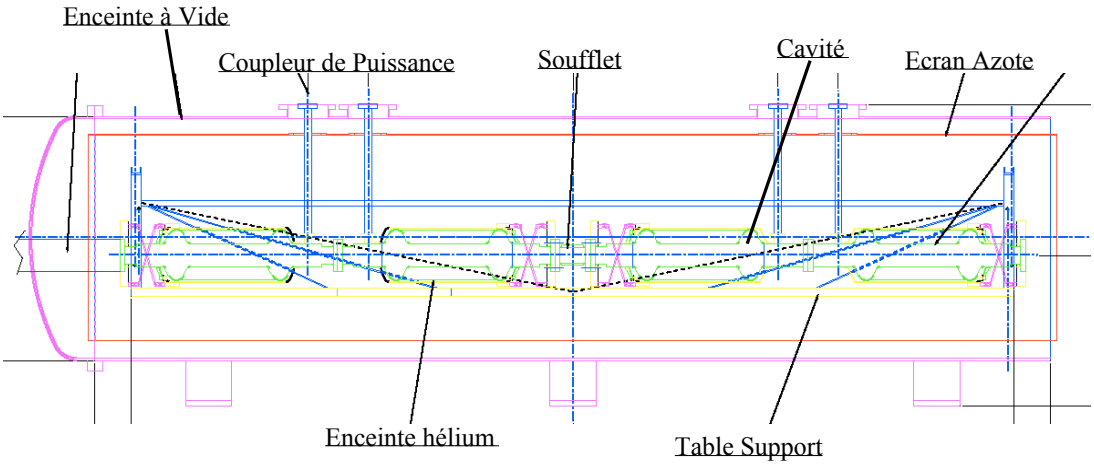

Longitudinal view of the cryomodule.

The assembly of cavities and couplers has to be done inside a class 100 clean room in order to avoid dust contamination. The assembly can be done outside the clean room provided the cavity/coupler ensemble is leak tight and sealed. The insertion in the cryomodule of the full 4-cavity assembly has to be done from the side.

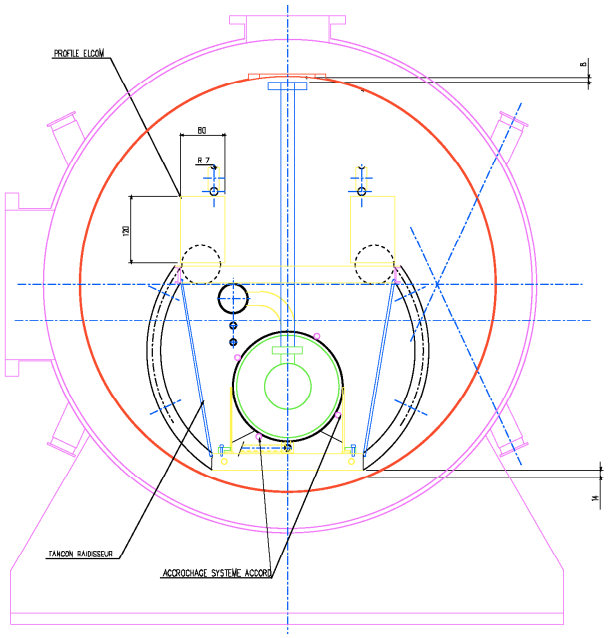

Front view of the cryomodule. The cavity is laid on a cooled table in a cradle shape structure on the bottom side of the helium vessel.

Power Coupler

The power coupler is an important (and weak) element bringing the RF power from room temperature down to the cold cavity. It should be stressed that even though the power level is rather low (5 kW), this item should be developed and fully tested during the TDS phase. If not, the overall schedule would shift as the power coupler is on the critical path. Moreover, in view of a future upgrade, it would be very interesting to check whether the power coupler could be designed

to withstand a CW power of 100 kW. Some basic parameters for the two options (5 kW & 100 kW) are described in Table II. Basically the external diameter should be higher for the high power operation to avoid the multipacting bands. The mechanical impact on the cryomodule mounting has also to be thoroughly analyzed. The TDS work should determine if a high power coupler could be safely implemented at that stage or not.

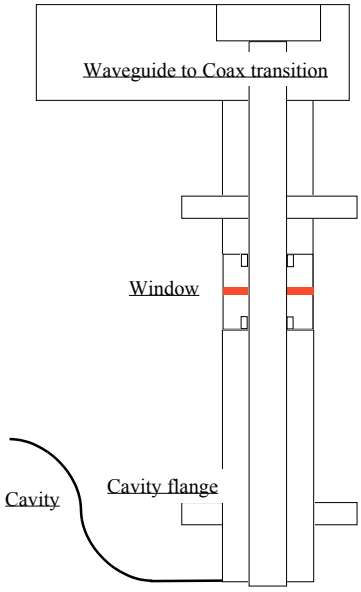

Schematic design of the coaxial coupler for SPIRAL II.

Parameter	5 kW	100 kW	
External Diameter (mm)	41.3 (standard 1"5/8)		80
Impedance (ohms)	50		
Internal Diameter (mm)	17.9		35
First Multipactor Barrier (kW)	125		1765
Total Dissipated power at 300K (W/m)	25.7	514	265
Inner Conductor Dissipated Power at 300K (W/m)	18	358	185
Outer Conductor Dissipated Power (W/m)	7.8	156	80
Inner Conductor Maximum Field (kV/cm)	0.95	4.23	2.18
Outer Conductor Maximum Field (kV/cm)	0.41	1.84	0.95

Dielectric Losses in the Window (W)	1.4	28	28
Inner Conductor Losses cavity side (W)	5.4	107	55
Thermal Gradient at the Window (K)	3.5	68.7	42

Table II –Coaxial power coupler parameters for both the 5 kW and 100 kW options.

RF Source

The RF power is a 5 kW CW klystron TH2466 from Thalès (formerly Thomson) company. A complete RF power source includes :

- The klystron tube (5 kW CW)
- A power supply (11 kV, 1.2 A)
- A waveguide WR650 circulator (5 kW any phase)
- A water power load WR650 (5 kW CW)
- Miscellaneous waveguide components, couplers, elbows, transitions, etc…

The RF tube could be installed right close to the cryomodule minimizing the length of waveguides and reducing the RF losses.

Low Level RF

SCRF cavities have to be regulated in frequency, field amplitude and phase. A precise regulation is required to maintain the cavity at the right frequency and the accelerating field at the right value and phase. The frequency is controlled using the cavity tuning system to better than 1Hz. It is generally a rather low speed (typically one second) when using the stepping motor. A high gain feedback loop for cavity phase and amplitude is necessary to compensate for mechanical vibration and microphonics. It should be possible to obtain with a properly designed phase lock loop a field control better than 1% and a phase control better than 0.1 degree. Each cavity has to be driven by a single RF power source. This is very important to guarantee the phase and amplitude control.

Beam Transport

The beam transport is rather simple taking in account the fact that a 45 MeV electron beam is highly relativistic (90). In particular, no specific focusing is required inside the cryomodules. Depending on the transport line length, only a few quadrupole triplets are really necessary. An intermediate analysis line could be useful in between the two cryomodules (at an energy of 5 MeV) in order to fully characterize the beam at the exit of the capture cavity.

Another quite interesting feature is the beam shaping on the target. Depending on the target size and shape, the beam spot can be moved using a pair of deviating magnets. This easily allows covering any area shape on the target. For example, an annular beam can be formed using only 0.05 T deviating magnets in the (xy) plane 90° out of phase and located 2.5 m away from the target. The corresponding beam envelope is calculated from the magnets to the target point(see below).

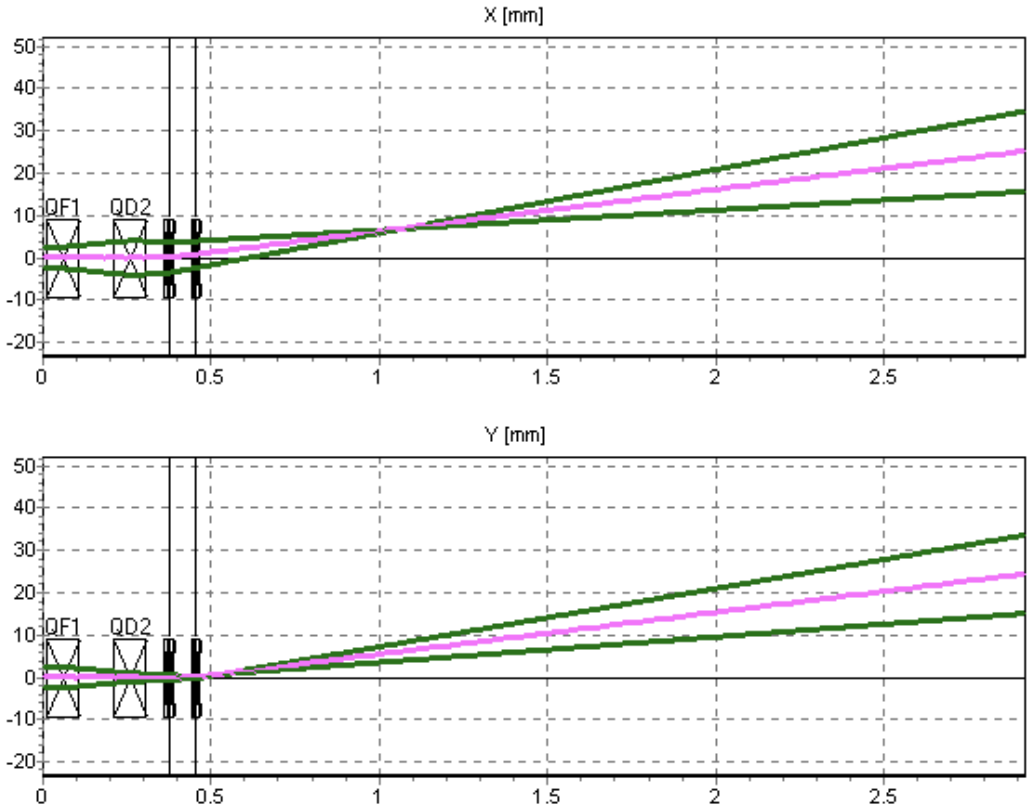

Beam envelopes using magnets to produce an annular beam on the target.

Cryogenic Plant

The required cryogenic power is of the order of 150 W at the working temperature of 1.9 K including the static losses, the power coupler losses and a standard margin. The Hélial 2000 liquefier from Air Liquide can fulfill these requirements. Using nitrogen pre-cooling, its performance can reach 130 l/h in the liquefying mode and over 400 W (@ 4.5 K) in the refrigeration mode. This liquefier has many interesting characteristics as the static gas bearing expansion turbines and the industrial oil lubricated screw compressor. It offers the remote monitoring from a distant location (control room) through a fully automated controller.

Although the liquefier is the major component of the cryogenic plant, the overall plant should include the liquefier (150 W @ 1.9 K), a large dewar, a helium compressor, a storage tank for helium gas, a pumping station, transfer lines for helium and nitrogen, a liquid nitrogen reservoir and all ancillary components : controller, gas purification, heater, etc…

Shielding

The electron accelerator has to be shielded from radiological gamma rays that may be produced upon beam losses especially in the beam dumps. This is the only radiological hazard, since no neutrons or protons are emitted, only gammas by Bremsstrahlung. A first set of calculation has been carried out to have a rough idea of what shielding would be required in order to achieve less than 0.5 □G/h (Note that this level corresponds to what will be required in the future for a non-

controlled (open) area) outside the accelerator area. The shielding will be primarily due to the high-energy beam dump losses (which are not yet defined). So the calculation assumes two variables : the losses in the beam dump (labeled i1) and the losses in the deviating magnet (i2). In any case, these losses are lower than the full beam current (500 μA).The figures below show the concrete thickness required in the front direction (called the primary wall) and perpendicular to the beam axis (secondary wall) using a regular concrete (of density 2.35 g/cm^3). In practice, a high-density concrete is generally used. In any case, this analysis shows that even in the extreme cases (where the shielding is designed assuming a full beam loss, which will never be the case), the primary wall would not exceed 3 m of high density concrete (or 5 m of standard) and the side walls less than 2 m. These figures will be reduced if one considers actual beam losses. In the same manner, the shielding has been evaluated along the transport beam line to the target area.

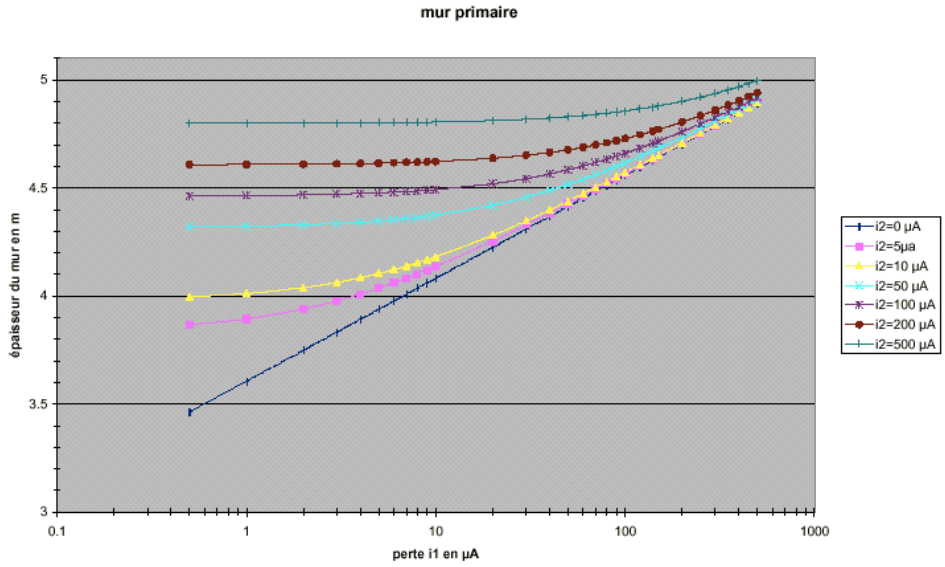

Thickness of the primary wall (regular concrete) as a function of beam current losses in the beam dump (i1) and in the bending magnet (i2) (upper). Same for the side wall (below).

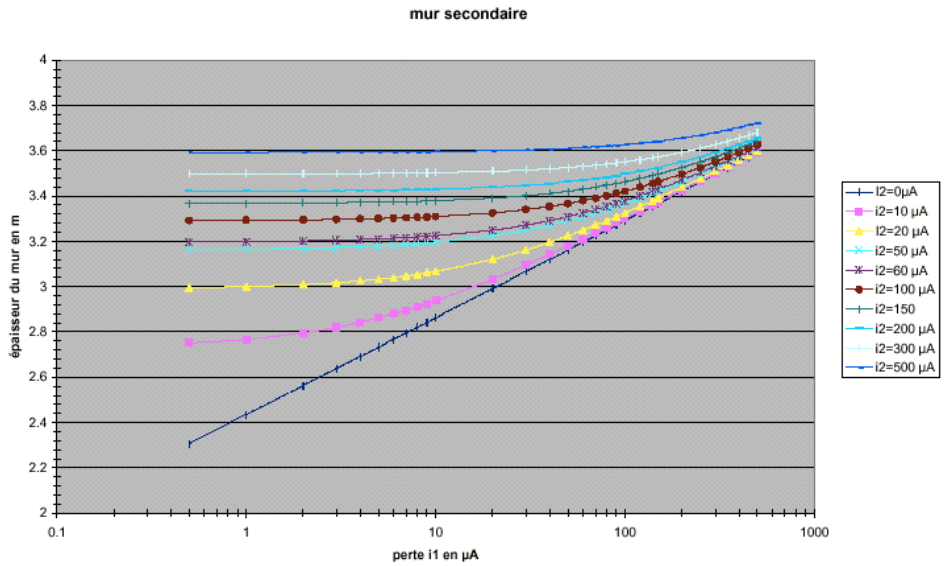

Control-Command

The proposed control-command for the driver accelerator can be done following a typical architecture used for large machines. A possible solution would be based on UNIX stations (Sun Ultra 5), VME based CPU relying on the EPICS software and VME interface cards. This solution is based on reliable technologies which are already implemented on many large equipment worldwide (DESY, LANL, etc…). The cryogenic system and the safety handling system would use each a specific controller, but some basic information will have to be shared with the control-command.

Diagnostics & Safety

Many diagnostics are needed in order to continuously keep the beam in control. The vacuum level at different locations should be permanently surveyed. Different other diagnostics like current monitors, gamma ray detectors, beam profilers, CCD cameras (light emission) and cryogenic diagnostics are also required.

For safety management, the beam current loss would be of primary interest (as seen from the above radiation analysis). Other safety trips may include radiation detectors, arc detectors and abnormal vacuum level.

Schedule

A high level schedule is shown in below (*after* completion of the TDS phase). First beam is expected within two years after the project construction kick-off but the final beam delivered to the target would be envisaged 3 years after project approval (assumed to be the starting point – January 2003).

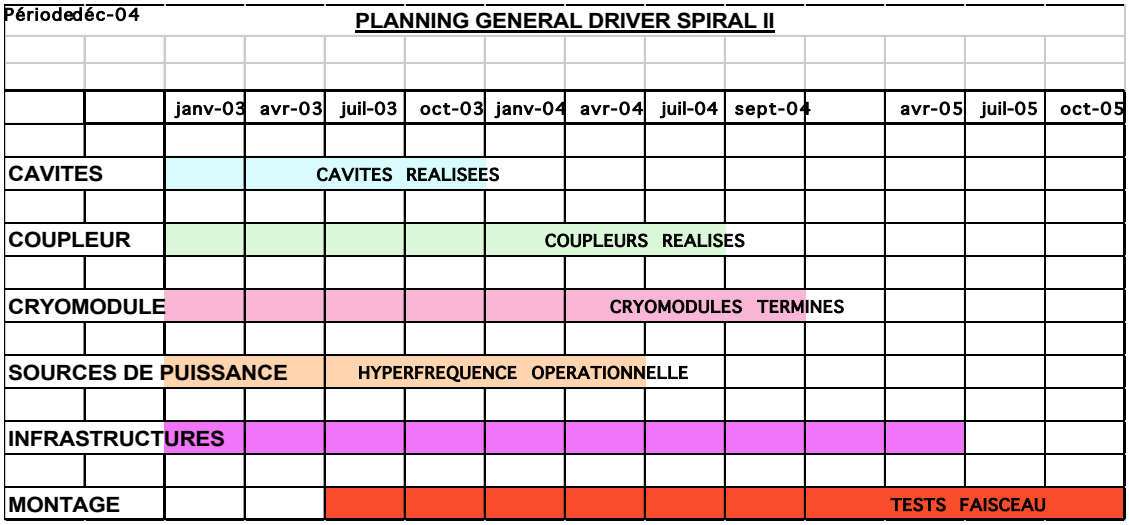

Schedule of the electron accelerator construction

.

The reference design of the electron driver accelerator for the SPIRAL II project is a superconducting linear accelerator. This allows continuous (CW) beam operation and a very high efficiency (100% RF to beam). It also enables to use low and cheap RF power sources and to make profit of superconducting radiofrequency (SCRF) cavities operating at high gradients. Moreover, it offers the possibility of easy upgrading.

A new option for a deuteron driver in the framework of the LINAG project. The Linag phase I

In the framework of the LINAG project [4], it is envisaged in a first phase to accelerate a deuteron beam at an energy of 40 MeV in an linear accelerator. This option is extensively described in the report mentioned before. Its cost will be studied in the last part of this document as well as the two other options.

SPIRAL II : Post-acceleration

The post-acceleration of RIBs produced by a new driver, other than the GANIL heavy ion cyclotrons raises the following questions :

- what is the energy range that can be reached in the cyclotron CIME by neutron-rich isotopes?
- if this range is too limited for the various fields of physics, is it possible :
  -to re-inject the beams issued from CIME into one of the SSCs ?
  -to inject the beam issued from the source into the entire series of GANIL cyclotrons, skipping CIME ?
- what is the best lay-out for the target + source cave in order to :
  - preserve the development of the present SPIRAL installation ?
  - feed a low energy beam line ?

Post-acceleration

Post-acceleration by CIME

It is to be remembered that the exotic ions exiting leaving the N+ source are in small number. Therefore, the operation point of the source must be chosen for the most probable charge state with the highest intensity. In what follows, we have considered that the source is a standard 14 GHz ECR and we have collected a series of experimental results (figure below) giving the

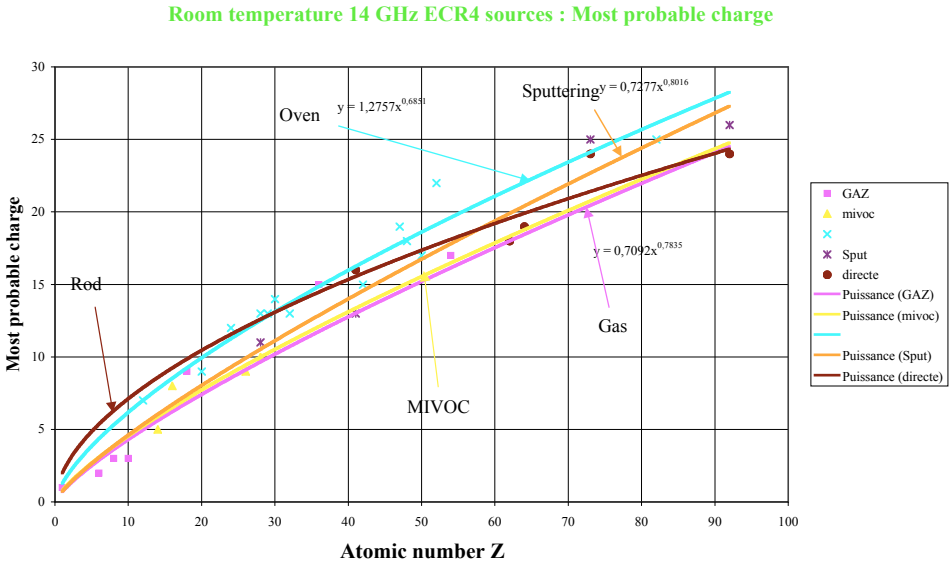

optimum charge state obtained by different methods, as a function of the atomic number of the ion species. It is then easy, at least for post-acceleration by a single cyclotron without stripping, to have a good image of the maximum attainable energy.

CIME was optimized for ion masses below 100. Around this value and higher, the following table indicates for some examples of neutron-rich isotopes, the maximum energy for the average charge state read on the previous figure .

Element	Z	A	Q average	W max (MeV/n)
Ni	28	68	13	9.6
Ni	28	78	13	7.3
Kr	36	90	15	7.3
Kr	36	94	15	6.7
Sn	50	128	18	5.2
Sn	50	132	18	4.9
Xe	54	140	20	5.4
Xe	54	144	20	5.0

For these projectiles bombarding for example C or Pb targets, the coulomb barrier ranges from 3 to 5 MeV/n. Therefore, physics in this vicinity is possible, but the available energy range is quite limited above.

Acceleration by CIME and the GANIL SSC

Cyclotrons operating with identical RF frequencies

In this situation, there exists a series of conditions of compatibility between RF harmonic modes, and magnetic and RF frequency ranges.

Only one case of direct re-injection of a CIME beam into an SSC is possible: CIME operating in harmonic mode 5 and SSC2 on harmonic mode 4. As seen on the CIME working diagram (figure below), this considerably restricts the operating range of CIME to a narrow band of injection energies $1.7 < W < 3.4$ MeV/n. This leads to CCS2 output energies ranging from 11 to 21 MeV/n and requires a solid stripper anyway.

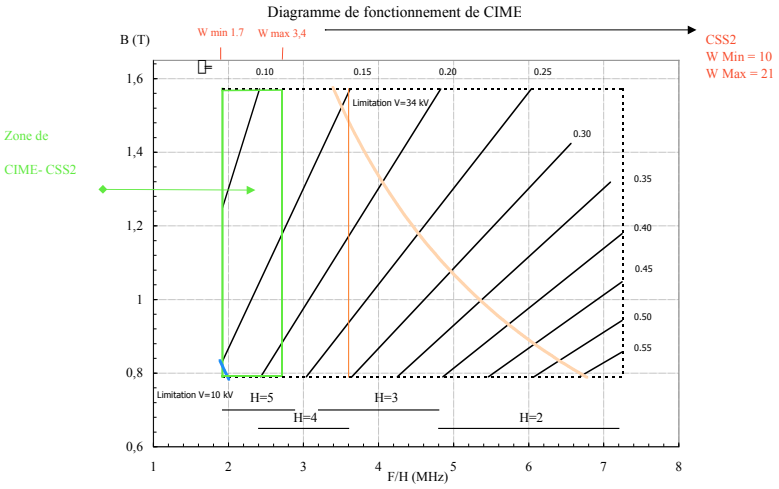

Any other case would require both stripping and energy degradation of the beam extracted from CIME (provided the mean charge state obtained after the degrader would fit the RF frequency conditions) , thus leading to a degradation of the beam characteristics and the resulting undesirable ion losses.

Cyclotrons operating with independent RF frequencies

Then, the beam bunches accelerated by CIME would have to be submitted to the following treatment :

- first, to be de-bunched over as close as possible to 360° by an RF cavity (C1) operating on the CIME RF frequency,
- second, to pass through a second cavity (C2) in order to reduce the energy spread generated by C1,
- third, to be re-bunched by a third cavity (C3) over ± 3° of the RF frequency chosen for SSC2.

As an illustration, in the case of $_{132}$Sn, C1 would have to provide a linear voltage of ± 1.7 MV with a risetime of 2.7 ns. Since it is doubtful that this were technically possible, a sine wave of at least twice this amplitude would be necessary in order to debunch with an efficiency of about 50 %. The second cavity C2 would have comparable requirements, while the third one C3 would have to deliver much stronger a voltage than the present rebuncher R2 since operating on a quasi-continuous beam. Adding to this the fact that C1 to C3 must be variable frequency cavities makes the job not foreseeable in a five-year period.

As a conclusion, re-injecting the beam from CIME into SSC2 covers an energy range from 11 to 21 MeV/n. If higher energies are needed, injection into the whole series of the GANIL cyclotrons is to be considered

Acceleration by the C0, SSC1 and SSC2

In order to reach energies higher than 21 MeV/n, the atoms produced in the fissile target would have to be ionized, then directed to the Co injection line (either C01 or C02) through a dedicated beam line and accelerated through SSC1 and SSC2 with the stripper in between. The maximum energies attainable would then be the classical ones, as indicated on the figure below

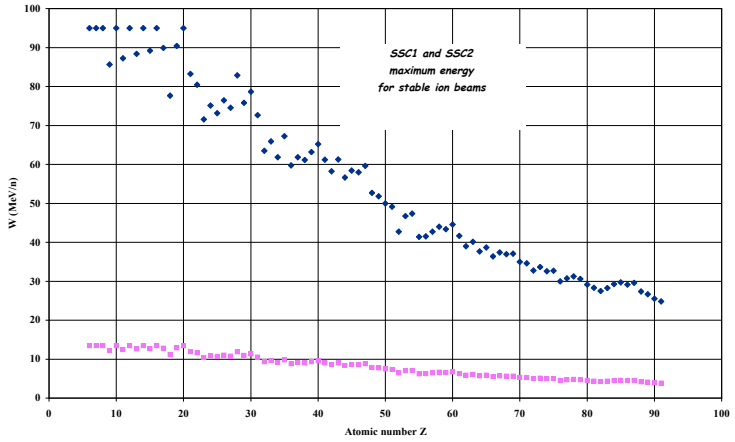

No basic calculations are needed in this case, only two choices have to be made for the transported beams :

- charge state : the roughly 150 m long beam path would be less expensive as regards the vacuum requirements (charge exchanges on the residual gas) if the beam were issued as 1+ ions from the source.
- energy : as will be seen in the next paragraph, the ions would have to run alongside the SSCs. The higher their magnetic rigidity, the less sensitive they would be to the SSCs leakage fields, therefore pleading in favor of a high extraction voltage from the ion source and (again) the lowest possible charge state.

Taking into account the fact that a new CIME central region can be designed for 65 kV, it seems sensible to direct the 1^+ ions toward the C01 high voltage platform. This would also make the beam line shorter and simpler as opposed to an injection into C02

Conclusion and final remark

Post acceleration by CIME of the radioactive beams generated through fission of uranium targets is limited to energies below 10 MeV/n. According to the ion species and to the possibility to go to higher charge states at the expense of the intensity, there might exist an energy gap between the CIME maximum energy and the SSC2 minimum one.

Energies above 21 MeV/n can be reached using the three GANIL cyclotrons as a post-accelerator. However, we want to stress the point that tuning and controlling several cyclotrons in a row for very small intensity beams is not at hand. No strong experience is acquired yet, even on a single cyclotron like CIME and this procedure seems very un-appropriate.

The postacceleration using CIME and the combination of CIME + CSS2 is therefore limited below 21 MeV/n as does not allow to cover the whole programme of physics described in the beginning of the report.

The possibility of adding to the SPIRALII project a linear post accelerator up to energies of 100 MeV/u is under discussion and consideration. This would allow to cover the wide programme of physics.

Implantation of SPIRAL II

The implantation of SPIRAL II has been devised by taking into account the main following options :

- The radioactive ions will be produced inside a specific cave, located at the west side of the GANIL accelerator building. The advantages are numerous, keeping free the second cave of the SPIRAL facility as a spare of the cave used at present or for the development of new techniques of ion production.
- The new SPIRAL II cave will be able to be built and commissioned without disturbing the SPIRAL functioning (otherwise, the adaptation of the SPIRAL cave 2 for SPIRAL II would have stopped the use of SPIRAL for a long time)
- A new cave will be able to be designed according to the SPIRAL II constraints, which would not have been the case with the SPIRAL cave 2 (lack of room, existing walls, presence of SPIRAL equipments)
- Taking into account the other projects planned in the near future around SPIRAL as the low energy beam facility (LIRAT) or the equiping of cave 2.

- Allowing to simultaneaous use most of the facilities. For instance, using LIRAT with the beam produced by the GANIL primary beam in the cave 1 and, simultaneously, providing experiment area with the beam coming from the SPIRAL II cave after accelerating in CIME.
- Keeping free room for future extensions such as a booster for CIME or a post-acceleration in CSS2
- Disturbing the functioning of the present facility as little as possible. For instance, keeping free the access to the accelerator hall for the trucks.

Technical options

Even if most of the technical options have no real influence on the implantation, a few must be taken into account .

- The principle of a two stage ionisation (mono-charge state source close to the production target followed by a charge breeder) has been chosen .
- A mass separator with the highest possible efficiency is suitable to purify the beam used by the low energy beam experiments and, also, to make easier the injection into CIME. A secondary output would be useful to provide simultaneously the low energy experiments with other type of ions. A low magnetic field dipole and a 30 kV source voltage could allow to reach an efficiency of 1000. The efficiency could be improved up to 2000 if the source voltage was increased to 60 kV (that imposes a platform). The room for a very high efficiency separator will be kept.
- The ions must be identified before injecting them into CIME. The present identification bench will be used, jointly with SPIRAL.
- The target will be vertically irradiated in order to simplify the safety problems.

Safety aspects

Up to now, few works have been carried out to evaluate the safety constraints and their influence on the SPIRAL II layout. The only data available today concern the safety of the electron linear accelerator (a 2m thick concrete wall around the accelerator seems sufficient) and the safety around the targets for deuterons (neutrons flux, fission products, ...).
One of the major problems not yet studied concerns the handling and the storage of the irradiated uranium targets. Our policy has been to keep open the different options, hoping that the room left free to install the equipments needed to respect the safety constraints would be sufficient. The detailed studies, carried out during the project design period, will allow to define these points precisely.

Implantation Proposal

The schemes below show the implantation proposed for the electron option and for the deuteron option (the linac tunnel is replaced by the cyclotron cave). The different parts of the facility are the following :

1. Linear accelerator in a tunnel. The electron energy, of 45 MeV in a first step, can be increased by increasing the cavity field. A 2 m thick roof covers the tunnel.
2. Linac gallery where the electronic devices (RF devices in particular) are installed.

3. Transit gallery to access to the linac gallery and to the LIRAT experiment area from outside. A crane allows to handle the equipments.
4. Electron beam damper.
5. Target and mono-charge state source at a bottom of a kind of well. The beam line is oriented vertically.
6. Secondary well to handle and extract out the target after irradiation.
7. Mass separator consisting in a low magnetic field dipole.
8. Free room for very high efficiency mass spectrometer.
9. Charge breeder.
10. Separator secondary output to provide the low energy experiments (LIRAT) with species not used by CIME.
11. Junction with the CIME injection line. The identification bench is adapted for use by SPIRAL I and II.
12. Existing SPIRAL cave 1
13. SPIRAL cave 2 not yet equipped. Probably, this cave will be equipped with a two stage ionisation system.
14. Low energy experiment area (LIRAT)
15. Free room to install a booster to post-accelerate the beam coming from CIME or directly from the target via a charge breeder.
16. Beam line to possibly transport ions from SPIRAL target to GANIL injector or from CIME to CSS2 in order to re-accelerate them.
17. Limit of an external building for services which could be an extension of the present SPIRAL building.

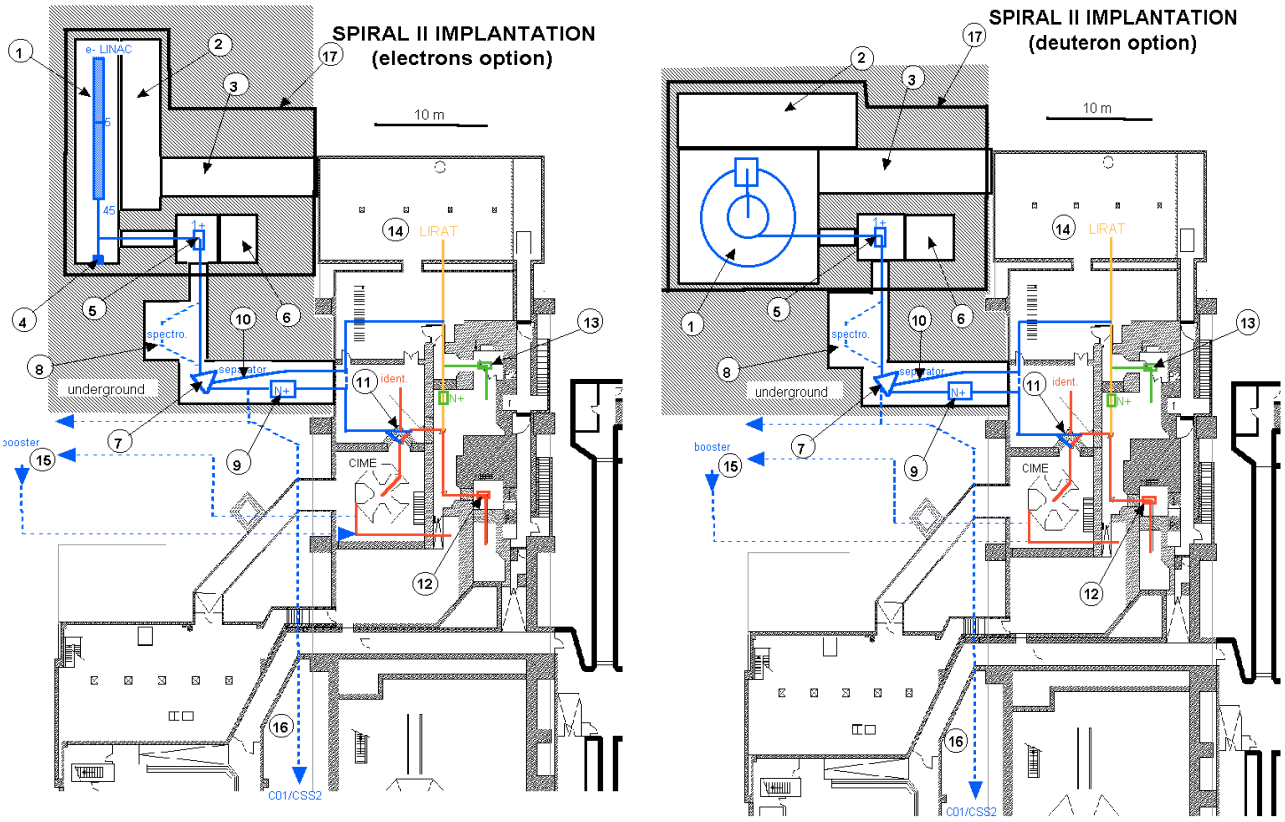

SPIRAL II Cost assessment

The cost of SPIRAL II has been devised by taking into account the main following options:

- The cost of the buildings has been deduced from the actual cost of the SPIRAL I building (about 2 k€/m^2). This building included an underground floor. For the cyclotron option, an underground floor is needed. For the linac options, the cost should be roughly the same with or without underground floor (the cost of the excavation is compensated by less radioprotection concrete). The basic networks and equipemnts (cranes...) are included.

- The cost of the target-source set and its infrastructures (caves, equipments, target handling system, target storage, ...), estimated at 3.2 M€, has been extrapolated from the cost of the SPIRAL I one (2 M€), taking into account that the target-source set of SPIRAL II will be larger, with more safety constraints. However, the cost of a target retreatment facility has been considered as an extra-budget (between 2 and 4 M€ according to the level of radioprotection regulation), the basic option being to store the targets without retreating them.
- The cost of the driver has been devised as follows :
  - Cyclotron for 80 MeV deuterons: Its price (12 M€) has been got from the european industry. It is valid for a turn-on-key cyclotron. This price could be reduced if some components are taken in charge by GANIL (deuteron source, control system for instance). A participation to the installation could reduce the price also.
  - Linear accelerator for 45 MeV electrons: The design and the construction will be carried on by French laboratories. The salaries of people working in these laboratories are not taken into account in the cost. Consequently, its price (6.1 M€) includes mainly the supplying of the components. Morever, the re-use of a part of MACSE (prototype of a superconducting linear accelerator built in Saclay) could reduce the cost (between 1 to 2 M€ could be saved).
  - Linear accelerator for 40 MeV deuterons: As for the electron linac, the design and the construction will be carried on by European laboratories, that means the salaries of people working in these laboratories are not taken into account in the cost and the price includes mostly the supplying of the components (18 M€). Moreover, the RFQ, pre-accelerating the beam going out from the source, is still in a conceptual design state. So, its price is not yet precisely estimated.

- The cost of the beam lines depends on their performances:
  - Beam lines from the driver to the target and from the target to CIME. These beam lines are as sophisticated as the SPIRAL I ones. So; the same price as for SPIRAL I will be retained for these lines (75 k€/m);
  - The 1/1000 separator has been estimated at 300 k€;
  - The price of the charge breeder is based on the market price of ECR sources (400 k€)
  - The beam line from the second separator output to the LIRAT line junction. This line is just a transport line. Its price is lower (40 k€/m);
  - The beam line from CIME to CSS2 is partly a sophisticated line and partly just a transport line. Its price reflects this fact (50 k€/m). The price of the corridor-like building to cover the line with radiologic protection must be added (1 k€/m2);
- The cost of the control-system is relatively low (300 k€) because the drivers are simple to control (constant energy, unique particule).
- The cost of the radioprotection is difficult to estimate. Indeed, up to now, there has been ere no real study of the constraints induced by the regulation, in particular concerning the use of uranium in the target. The price which is proposed (1.5 M€) is just an extrapolation of the cost of the radioprotection for SPIRAL I (1 M€), without taking into account further constraints like a confining vessel around the target.

- Few further expenses have been taken into account like travels (0,15 M€), site roads, car parks and green areas (0,15 M€).
- A sum of 10 % of hazards has been added.

Estimation of the cost

In the next page, is given the estimated cost in millions of Euros (M €)

SPIRAL II BUDGET			
(M€)	**40 MeV deuteron linac**	**45 MeV electron linac**	**80 MeV deuteron cyclotron**
Building / Infrastructure	5,6	3,2	4,3
Driver	18,6	6,2	12,2
Targets / Sources 1+	3,2	3,2	3,2
Source N+	0,4	0,4	0,4
Beam lines	4,6	4,3	4,3
Radioprotection	1,5	1,2	1,5
Control system	0,3	0,3	0,3
Miscellaneous	0,3	0,3	0,3
Hazards (10%)	3,5	1,9	2,6
TOTAL (M€)	38,0	21,0	29,1
MACSE re-use		-2,3	
GRAND TOTAL (M€)	**38,0**	**18,7**	**29,1**

target retreatment	3,0
CSS2 re-acceleration	4,4

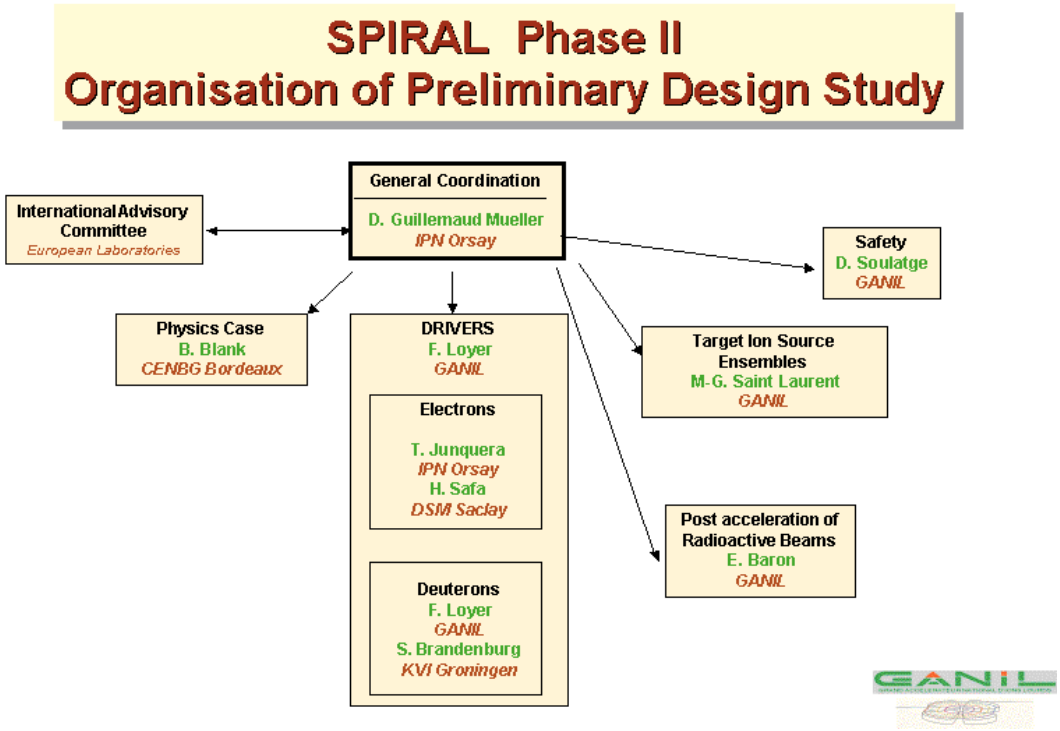

In the following, one will find the list of the people involved in the Preliminary Design Study of SPIRAL II.

International Advisory Committee

G. de Angelis (INFN Legnaro), S. Brandenburg (KVI Gröningen), Ph. Dessagne (IReS Strasbourg), J.P. Gatesoupe (DSNQ/MSN CEA Saclay), W. Gelletly (University of Surrey), M. Huyse (KU Leuven), B. Jonson (Göteborg), J. Martino (SPhN/DAPNIA Sacla), W. Mittig (GANIL Caen), Yu. Ts. Oganessian (JINR Dubna), M. Schädel (GSI Darmstadt), R. Julin (Jyväskylä)

Physics Case

F. Auger (Saclay), J.F. Berger (Bruyères le Châtel), B. Blank (CENBG Bordeaux), M.J.G. Borge (Madrid), A. Bracco (INFN), M. Chartier (CENBG Bordeaux), P. Roussel-Chomaz (GANIL), P. Dessagne (IreS Strasbourg), M. Girod (Bruyères le Châtel), S. Grévy (LPC Caen), F. Gulminelli (LPC Caen), M. Hellström (GSI Darmstadt), W.Korten (Saclay), D. Lacroix (LPC Caen), D. Lunney (CSNSM Orsay), M. Marques (LPC Caen), G. Neyens (KU Leuven), J.A. Pinston (ISN Grenoble), M. G. Porquet (CSNSM Orsay), N. Redon (IPN Lyon), P.H. Regan (University of Surrey), O. Sorlin (IPN Orsay), C. Stodel (GANIL), C. Volpe (IPN Orsay), J.P. Wieleczko (GANIL)

Target-Ion source ensembles

N. Chauvin (CSNSM Orsay), S. Essabaa (IPN Orsay), F. Ibrahim (IPN Orsay), P. Jardin (GANIL), U. Koester ISOLDE), D. Ridikas (Saclay) H. Safa (Saclay), T. Lamy (ISN Grenoble), M G Saint Laurent(GANIL), ACC. Villari (GANIL)

Deuteron driver

F. Loyer (GANIL), S. Brandenburg (Gröningen)

Electron driver

J.L. Biarrotte (IPN Orsay), P. Blache (IPN Orsay), L. Bourgois (Saclay), C. Commeaux (IPN Orsay), G. Devanz (Saclay), J.F. Gournay (Saclay), M. Jablonka (Saclay), T. Junquera (IPN Orsay), M. Lamendin (Saclay), M. Luong (Saclay), N. Pichoff (Saclay), M.Poitevin (Saclay), H. Safa (Saclay), H. Saugnac (IPN Orsay), C.Travier (Saclay)

Postacceleration of radioactive beams

E. Baron (GANIL), F. Chautard (GANIL), D. Jacquot (GANIL, F. Varenne (GANIL)

References

[1] Spiral II European RTT contract number ERBFMGECT980100, M.G. Saint Laurent, G. Lhersonneau, J. Aystö, S. Brandenburg, A.C. Mueller, J. Vervier

[2] C. Lau, PhD, University Paris 7, IPN Orsay T 00 08 (2000)
N. Pauwels, PhD, University Paris Sud, IPN Orsay T 00 12 (2000)
F. Clapier et al., Phys. Rev.ST Accelerator and beams, 1 (1998) 013501
F. Ibrahim et al. Submitted to Euro. Phys. Journal
B. Roussiére et al. Submitted to NIM

[3] Module Accélérateur de Cavités Supraconductrices à Electrons, Internal Report DAPNIA/SEA 92-09, 1992

[4] High intensity beams at GANIL and future opportunities : LINAG, G. Auger, W. Mittig, M.H. Moscatello, A.C.C. Villari Ganil Report R01 02